



Cite this: *Lab Chip*, 2022, **22**, 1852



Received 22nd December 2021,  
Accepted 11th April 2022

DOI: 10.1039/d1lc01160j

rsc.li/loc

## Electrically-driven handling of gametes and embryos: taking a step towards the future of ARTs

Adriana Karcz, <sup>\*ab</sup> Ann Van Soom, <sup>b</sup> Katrien Smits, <sup>b</sup> Rik Verplancke, <sup>a</sup> Sandra Van Vlierberghe <sup>c</sup> and Jan Vanfleteren <sup>a</sup>

Electrical stimulation of gametes and embryos and on-chip manipulation of microdroplets of culture medium serve as promising tools for assisted reproductive technologies (ARTs). Thus far, dielectrophoresis (DEP), electrorotation (ER) and electrowetting on dielectric (EWOD) proved compatible with most laboratory procedures offered by ARTs. Positioning, entrapment and selection of reproductive cells can be achieved with DEP and ER, while EWOD provides the dynamic microenvironment of a developing embryo to better mimic the functions of the oviduct. Furthermore, these techniques are applicable for the assessment of the developmental competence of a mammalian embryo *in vitro*. Such research paves the way towards the amelioration and full automation of the assisted reproduction methods. This article aims to provide a summary on the recent developments regarding electrically stimulated lab-on-chip devices and their application for the manipulation of gametes and embryos *in vitro*.

### Introduction

Infertility is a condition which affects couples around the world regardless of gender, race or nationality.<sup>1–3</sup> The underlying causes of subfertility can be distinguished into male<sup>4–7</sup> and female<sup>8–12</sup> factors. Reduced fecundity can significantly affect our daily life and thus be considered as a marker of general health. Both infertile men and women are likely to have comorbidities (such as increased risk of

<sup>a</sup> Centre for Microsystems Technology (CMST), Imec and Ghent University, Technologiepark Zwijnaarde 126, 9052 Zwijnaarde, Ghent, Belgium.

E-mail: adriana.karcz@gmail.com

<sup>b</sup> Reproductive Biology Unit (RBU), Faculty of Veterinary Medicine, Department of Internal Medicine, Reproduction and Population Medicine, Ghent University, Salisburylaan 133 D4 entrance 4, 9820 Merelbeke, Belgium

<sup>c</sup> Polymer Chemistry and Biomaterials Group, Centre of Macromolecular Chemistry, Ghent University, Campus Sterre, building S4, Krijgslaan 281, 9000 Ghent, Belgium



**Adriana Karcz**

Adriana Karcz is a PhD candidate at CMST (Centre for Microsystems Technology), Imec and Ghent University, and Faculty of Veterinary Medicine at Ghent University, Belgium. She is working on the development of a digital microfluidic platform for the *in vitro* manipulation of mammalian embryos. The project involves active participation in two distinct fields of study, *i.e.*, micro- and nanotechnology engineering and reproductive medicine. Her research focuses on the adaptation of standard bioprotocols for the on-chip manipulation of cells and biofluids with the use of electric fields.



**Ann Van Soom**

Prof. Dr. Ann Van Soom holds a position as full professor at the Faculty of Veterinary Medicine, Ghent University, Belgium. She is investigating *in vivo* embryo-maternal and *in vitro* embryo and culture environment interactions in domestic animals. Additionally, she focuses on more applied research in cryopreservation of gametes and embryos, the identification of markers for embryo quality/pregnancy outcome in humans and the development of a microfluidic system in collaboration with the engineering department. She was elected as board member of the International Embryo Technology Society and a member of the EU-ITN network RepBiotech, and is now involved in EU-ITN network Eurova.

different types of cancer and cardiovascular and metabolic diseases).<sup>13,14</sup> Numerous studies have shown that subfertility causes psychological distress, depression, anxiety and may lead to the abuse of stimulants among women.<sup>14</sup> There is no doubt that both men and women are more susceptible to develop mental health problems. However, psychological therapy proved to be an efficient tool to reduce these harmful effects of infertility on patients.<sup>15</sup> Therefore, the reassurance of comprehensive fertility care is essential. "Assisted reproductive technologies" (ARTs) stand for a group of procedures developed to facilitate conception that would result in the birth of a healthy offspring, which would otherwise be difficult or impossible to achieve by natural intercourse. An ART cycle involves hormonal stimulation of ovaries, egg retrieval, *in vitro* maturation (IVM), *in vitro*

fertilization (IVF) or intracytoplasmic sperm injection (ICSI), *in vitro* embryo culture (IVC), embryo transfer (ET) and eventually cryopreservation of gametes and embryos. Additionally, ARTs may offer preimplantation genetic diagnosis (PGD) and preimplantation genetic screening (PGS) which allow for the assessment of the genetic disease potential of an early embryo before transfer. For more detailed definitions of the terms used, we kindly refer the reader to "The International Glossary on Infertility and Fertility Care, 2017".<sup>16</sup> The development of ARTs has a long history. Numerous studies contributed to the creation of current procedures which eventually led to the birth of the first healthy human child after a successful IVF.<sup>17,18</sup> Since then, multiple efforts have been made to improve the conditions of *in vitro* production (IVP) of mammalian



**Katrien Smits**

*Katrien Smits obtained her PhD in Veterinary Sciences from Ghent University in 2010. Presently, she is assigned as professor of equine assisted reproduction at the Faculty of Veterinary Medicine, Ghent University. Her research focusses on assisted reproduction and embryo-maternal interaction in horses and she specializes in cryopreservation (vitrification) and intracytoplasmic sperm injection (ICSI) techniques. The*

*fruits of her work are the birth of SMICSI, the first test tube foal born in Belgium, and VISCI, the first foal born from a vitrified, immature oocyte in the world. She runs a clinical lab, performing around 250 equine ICSI-cycles per year.*



**Sandra Van Vlierberghe**

*Prof. Dr. Sandra Van Vlierberghe holds a guest professorship at Vrije Universiteit Brussel (VUB) and a full professorship at Ghent University (Polymer Chemistry & Biomaterials Group, Belgium). She has acquired expertise related to the synthesis, the modification and the processing of (bio)polymers including thermoplasts (e.g. polyesters) and hydrogels (e.g. proteins and polysaccharides) for a variety of tissue engineering applications.*

*She is experienced in the field of polymer processing using 3D printing, electrospinning and two-photon polymerization (2PP). In 2017, she received the Jean Leray award from the European Society for Biomaterials.*



**Rik Verplancke**

*Dr. ir. Rik Verplancke obtained the academic degree of doctor of electrical engineering from the Electronics and Information Systems department, Ghent University (Belgium) in 2013. In his PhD, he developed a generic technology platform for the integration of microelectronics and microfluidics on stretchable substrates. Since 2013, he has worked as a postdoctoral researcher at the UGent/IMEC-CMST (Centre for Microsystems*

*Technology) group. His research focuses on the development of new thin-film based technologies for hybrid, mechanically deformable/stretchable electronic systems and polymer-based microsystem technologies in general.*



**Jan Vanfleteren**

*Prof. Dr. ir. Jan Vanfleteren obtained his PhD in electronic engineering from Ghent University, Belgium, in 1987. He is currently a Principal Member of Technical Staff at UGent/IMEC/CMST (Centre for Microsystems Technology) group and is involved in the development of novel interconnection, assembly and substrate technologies, especially in wearable electronics and polymer microsystem technologies. In 2004 Jan Vanfleteren was*

*appointed as part time professor at Ghent University and since 2009 he has been a promoter of 20 successfully defended PhDs. He is (co)-author of more than 200 papers in international journals and conferences with a H-index of 30.*



embryos. Most of them, however, were directed towards the optimization of the environment surrounding the embryo, such as the culture medium composition and the conditions kept inside the incubator.<sup>19</sup> Despite the fruitfulness of these attempts, the developmental rates of IVP embryos are still suboptimal and species-specific. For instance, in mice<sup>20</sup> and cows,<sup>21</sup> the amount of embryos that reach the blastocyst stage upon standard IVC, is 80–90% and 20–40%, respectively. In pig IVP, 80% of oocytes fertilized by a single sperm can grow into blastocysts, however, the high incidence of polyspermic fertilization up to 70% significantly lowers the success rates of swine IVP.<sup>22</sup> Until now, no protocol was proposed for horses due to the lack of success in equine IVF,<sup>23</sup> but equine ICSI is possible.<sup>22</sup> Introduction of proteins present in biofluids collected from the pig reproductive tract in swine embryo IVC<sup>24,25</sup> and extracellular vesicles isolated from the bovine follicular and oviductal fluids in bovine IVC<sup>26</sup> resulted in a higher percentage of blastocysts<sup>24,26</sup> or avoidance of genetic aberrations.<sup>25</sup> Thus, decreased rates of mammalian IVP can be related to the absence of the maternal genital tract and its functionality. Moreover, mammalian embryos communicate with each other and their surroundings when cultured in groups *in vitro*.<sup>27</sup> These findings clearly highlight the importance of the early embryo microenvironment, both *in vivo* and *in vitro*.<sup>28,29</sup> *In vivo*, the mammalian oviductal epithelium consists of two types of cells, which determine its function. Ciliated cells (together with the smooth muscles of the uterine tube) are responsible for the transport of gametes and embryos, while secretory cells provide them with essential nutrients.<sup>30</sup> *In vitro*

maturation reflects the time when the cumulus oocyte complex (COC) is released from the ovarian follicle and picked up by the fimbriae. *In vitro* fertilization attempts to reciprocate the situation occurring in the ampullary region of the oviduct, *i.e.* the co-incubation of gametes upon which a single sperm cell fuses with the ovum creating a zygote. *In vitro* culture corresponds with the period during which the embryo develops further while being moved along the isthmus towards the uterus, where it will eventually implant. The formulation of an early embryo consists of a cascade of events steered by the interactions between the gametes, the embryo and their surroundings.<sup>31</sup> Therefore, the IVM, IVF and IVC protocols need to satisfy the requirements supporting the stimulation of gametes and subsequent cellular divisions and reprogramming of the resulting zygote until it transforms into a blastocyst and can be transferred into the womb. A schematic representation of the mammalian oviduct and its significance in the early embryonic development *in vivo* with related *in vitro* techniques are shown in Fig. 1.

The success rates of human ARTs are fairly difficult to analyse due to the amount of contributing variables. IVF is a costly procedure with the price per cycle varying between countries.<sup>32</sup> The accessibility and utilization of these procedures are related to cultural aspects, government regulations, religious beliefs and socioeconomic status.<sup>33–36</sup> The global live birth rate calculated as the percentage of the total number of ART cycles using autologous oocytes (fresh and cryopreserved) based on the data collected in Australia, New Zealand, Canada, Continental Europe, UK, Japan, Latin

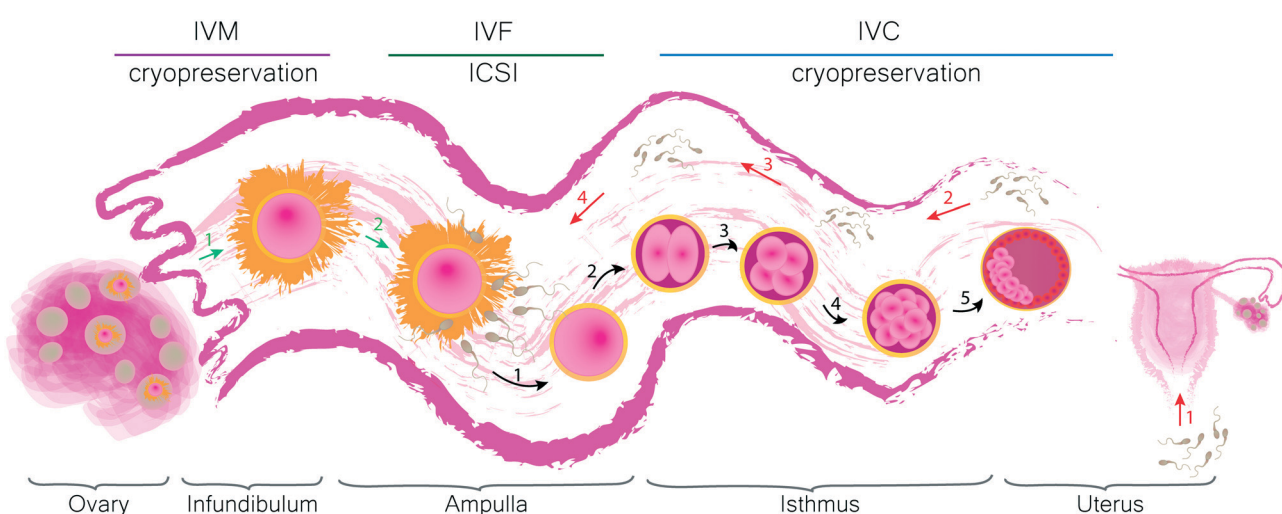


**Fig. 1** Importance of the mammalian oviduct and *in vitro* methods in assisted reproduction: IVM, IVF, ICSI, IVC, and cryopreservation of gametes and embryos. Sections of the uterine tubes: infundibulum, ampulla and isthmus are shown. Green arrows: 1) cumulus-oocyte-complex (COC) is picked up by the fimbriae of the infundibulum and 2) transported to the ampulla. Red arrows: 1) spermatozoa is deposited into the uterus during coitus and (2–4) travels through the lumen of the oviduct to the ampullary region creating a sperm reservoir. There, a single sperm cell fuses with the COC and fertilization occurs. Black arrows: 1) a resulting zygote is moved towards the uterus undergoing subsequent cellular divisions, 2) from 1-cell to 2-cell, 3) 4-cell to morula, 5) until a blastocyst. Red cells surrounding the blastocoele (blastocyst cavity) represent the trophoblast which will contribute to the creation of placenta. Clustered pink cells depict the inner cell mass (embryoblast) which will differentiate into the structures that will further develop into a foetus. Thinning of zona pellucida (protective coat surrounding the oocyte and embryo, here: yellow) during early embryonic development is shown.



America and USA between the years 2004 and 2013 adds up to around 20.5%.<sup>37</sup> A decline in live birth rates (after fresh IVF or ICSI cycle), however, was later observed and was related to more pronounced utilization of practices added in recent years, for example the elective single embryo transfer (eSET), and progressing industrialization and commoditization of ARTs.<sup>38</sup> The optimization of single embryo culture conditions *in vitro* could improve the birth rates after single embryo transfer (SET) and decrease the number of embryos produced *in vitro*. This could result in the reduction of embryo cryopreservation and thereby increase the utilization by lowering the cost of one IVF cycle.<sup>39</sup>

Besides the above-mentioned issues, risks linked to ART treatments exist.<sup>40,41</sup> Threats posed by multiple pregnancies

to both the developing foetus(es) and the mother are known<sup>42,43</sup> and some malformations have been linked to IVF treatments.<sup>44</sup> Furthermore, children born after assisted reproductive procedures have distinct epigenetic profiles as compared to children conceived in a natural way.<sup>45,46</sup> Changes in the epigenomes among various mammalian species are associated with the conditions of IVC.<sup>47</sup> Providing a suitable *in vitro* microenvironment that would better recreate the *in vivo* surroundings of an embryo could possibly reduce these genetic alterations. Therefore, the necessity to revise ART protocols that are currently in place in accordance with the state-of-the-art technologies in human and animal IVF and IVP is apparent. Preservation of endangered species by ARTs and research disciplines that are using *in vitro*

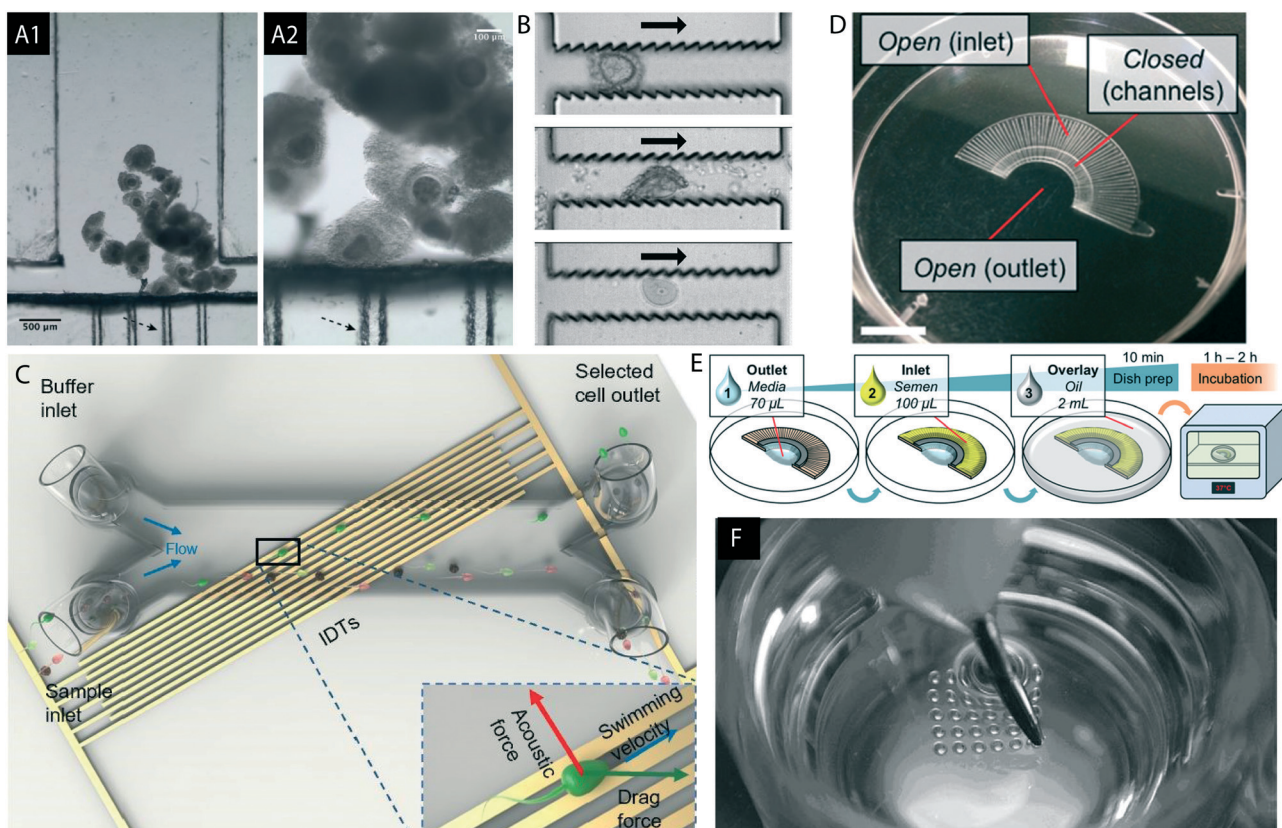


**Fig. 2** (A) Microfluidic chamber for the *in vitro* maturation of bovine oocytes is shown. Black arrows indicate the “filter-like” capillaries created to trap the cumulus oocyte complexes (COCs). The device was fabricated with the cyclic olefin copolymer using hot embossing and micromilling techniques which can be performed in a rapid manner outside of the clean room environment. Reproduced from ref. 72 with permission from SAGE. (B) Jagged PDMS microstructure for the purpose of stripping of the cumulus cells surrounding the mouse oocyte. Denudation of the ovum is a step prior to the injection of a sperm cell during ICSI, usually achieved by exposing the COCs to hyaluronidase followed by pipetting, or vortexing. The microdevice can serve as an alternative to the manual process. Reproduced from ref. 73 with permission from Royal Society of Chemistry. (C) Microfluidic PDMS channel mounted on top of a surface acoustic wave (SAW) chip for sperm selection. The acoustic field is generated using interdigital transducers (IDTs) while the semen sample flows through the channel. Both acoustic and drag forces are utilized for the selection of good quality and highly motile sperm. Reproduced from ref. 74 with permission from Royal Society of Chemistry. (D and E) FertDish developed for the selection of motile spermatozoa and ICSI in one dish. (E) FertDish process flow: the channels are filled with polyvinylpyrrolidone media and semen sample. The dish is next covered with oil and placed in the incubator giving time for the motile spermatozoa to pass through the microchannels towards the centre of the dish. Its architecture allows for the placement of droplets containing denuded oocytes for rapid single sperm selection and injection. Reproduced from ref. 75 with permission from Royal Society of Chemistry. (F) Well-of-the-well system (WoW), a microfabricated culture dish in mammalian IVC. It consists of an array of microwells located in the centre, each to be filled with a single embryo. Such structure allows for the exchange of paracrine and autocrine factors between the embryos and diffusion of waste products of metabolism in the culture medium. Reprinted from ref. 76 with permission from Elsevier.



culture at some point, such as aquaculture, parasitology and microbiology, could benefit greatly from the use of (digital) microfluidic devices (with faster application and biochip validation).

## Microfluidics

Microfluidics is gaining increasing interest in the field of mammalian reproduction. It refers to the study of the behaviour of fluids at a microscale where the predominant liquid-driving phenomena are related to the pressure gradients and capillary effects which arise within microchannel structures as well as the interactions occurring at the interface between two phases (liquid, solid, gas). Additionally, the fluids, as well as the particles suspended within, can be manipulated by the application of external stimuli in the form of electric and magnetic forces or acoustic waves.<sup>48</sup> Microfluidic chips designed for use in ARTs are plentiful and have been subjected to a number of reviews in the past 5 years.<sup>49–61</sup> Due to the high compatibility of sperm for its manipulation within microstructures, a plethora of such chips solely for the collection, handling and analysis of semen have been proposed and discussed.<sup>62–71</sup> Examples of microfluidic chips developed for the *in vitro* processing of oocytes,<sup>72,73</sup> sperm cells<sup>74,75</sup> and the culture of embryos<sup>76</sup> are presented in Fig. 2. Furthermore, processing of reactants for cryopreservation<sup>77</sup> as well as isolation and characterization of biomarkers of embryo quality<sup>52</sup> can be achieved using microchannels. Microfluidics was employed to study the embryo mechanics while hydrogel microchannels mimicking the stiffness of the oviduct's epithelium were used to provide a mechanical model for mouse embryo hatching out of the zona pellucida, which forms a protective coat surrounding the oocyte and embryo.<sup>78</sup> Based on the mechanical properties of an early human zygote, a prediction of the oocyte's developmental competence can be made.<sup>79</sup> Confinement of gametes and embryos within microchannels allows for more focus to be given to physical and mechanical stimuli *in vitro* to better mimic the *in vivo* situation.<sup>51</sup> Culture medium droplets of reduced sizes yielded better results in blastocyst development of human embryos.<sup>80</sup> Additionally, an IVP embryo is subjected to stress induced by various assisted reproductive procedures.<sup>81</sup> It was shown that human and mouse early embryonic development is adversely affected by the gradients of metabolism products, such as ammonium, suggesting the need for its removal from the culture medium.<sup>82</sup>

The benefits of microfluidics include significant reduction of reagent consumption, feasibility of usage, possible integration with other techniques, rapid fluid manipulation, closer recreation of microphysiological structures and real-time monitoring of the processes. Although the list of advantages can be further expanded with the growing application field, microfluidic technology has its downsides. These include complex operation and fabrication, the necessity for standardization of novel protocols, the difficulty

of translation to mass production and the requirement of additional equipment, *i.e.* for the fabrication of microstructures, but also for the operation, *e.g.* pumps for the medium supply as well as various microfluidic setup components such as tubing, connectors and alike. Some of these drawbacks, however, can be overcome by entering the field of digital microfluidics (DMF). The principal operation of DMF microdevices lies in the programmable manipulation of discrete droplets on an array of insulated electrodes on a chip.<sup>83</sup> The design of the electrodes determines the direction of droplet motion, creating virtual microfluidic channels excluding the requirement for external pumps and tubing. Moreover, the operation is fully programmable enabling faster translation and automation of standard laboratory protocols. Inclusion of digital microdevices in the workflows would not require extensive training of the personnel as most of the manual operations are replaced by the software, thereby minimizing the occurrence of human factor mistakes. This article aims to present the existing solutions based on the use of electric fields for *in vitro* cell and microdroplet processing in ARTs. The benefits and challenges of their application in assisted reproduction are debated on in the Discussion section.

## Electric fields in ARTs

Microdevices allowing for the handling and analysis of mammalian gametes and early embryos *in vitro* by means of an applied electric field utilize the phenomena of dielectrophoresis (DEP) and associated electrorotation (ER) as well as electrowetting on dielectric (EWOD). DEP has been widely exploited in various bioapplications such as nano- and microparticles' processing and manipulation of cells, including cancer and stem cells, viruses, yeast and bacteria, DNA or other biomarkers.<sup>84–86</sup> Additionally, DEP proved useful for the separation of bioparticles from complex biological samples, including sperm cells in forensic sciences.<sup>87</sup> EWOD microsystems have been applied in liquid lenses, in display technology, as DNA and (bio)chemical reactors, in diagnostics, immunoassays and cell culture<sup>88–91</sup> and a number of companies offer DMF solution in these sectors of technology.<sup>92</sup> The great advantage is the possibility towards the fabrication of portable devices which can be translated into mobile lab-on-a-chip (LoC) and point-of-care (PoC) microsystems.<sup>93,94</sup> Moreover, the possibilities of DMF applications seem unlimited as these devices are ready-to-use, both within and beyond the laboratory environment, and more of these point-of-use tools are continuously being developed.<sup>95</sup> Companies like digi.bio (<https://digi.bio>) and sci-bots (<https://sci-bots.com>) offer technical support in the translation of chemical and biological protocols onto the device along with the software and the chips. OpenDrop (<https://gaudi.ch/OpenDrop/>) is an open source DMF platform which can be adapted to fit specific research purposes. Recently, the instrument was transformed to enable the remote control of microdroplets onto the chip for



glucose detection and protein synthesis.<sup>96</sup> Such efforts pave the way towards the automation of often complex laboratory workflows which are time-consuming and require a lot of manual interventions.

Research articles covering microdevices developed for the *in vitro* manipulation and assessment of gametes and embryos with DEP and ER in the last decade (2010–2020) and with EWOD (2009–2020, including an application for the *in vitro* handling of a non-mammalian embryo) were analysed. In general, DEP and EWOD chips can be manufactured with the same materials and techniques that are common for the fabrication of microelectromechanical systems (MEMS). Printed circuit boards (PCBs) or glass serve as substrates on top of which metal (for instance gold, platinum, chromium, and copper) electrodes are deposited or patterned by means of photolithography followed by wet or dry etching. Indium tin oxide (ITO) is an alternative conductive material used in the fabrication of transparent microchips.<sup>91</sup> Vapour or atomic layer deposition techniques can be used for the application of insulating dielectric coatings (such as parylenes,<sup>97</sup> SiO<sub>2</sub>, Si<sub>3</sub>N<sub>4</sub> and metal oxides including Al<sub>2</sub>O<sub>3</sub>, HfO<sub>2</sub>, and Ta<sub>2</sub>O<sub>5</sub>, among others).<sup>98</sup> Spinoating is used to deposit functional coatings like polymer dielectrics (e.g. polydimethylsiloxane (PDMS), poly(methyl methacrylate) (PMMA), SU-8)<sup>91,99</sup> as well as fluoropolymers which serve as hydrophobic layers (Teflon, Cytop, Fluoropel).<sup>100</sup> Information about the materials used for the construction of chips considered herein along with the objectives, methods, main findings and species are listed in Tables 1–4. The configuration of the chip and the cell type determine the strength of the applied electric field required for cell and microdroplet motion.

### Dielectrophoresis and electrorotation

Dielectrophoresis is an electrokinetic phenomenon first described by Herbert Pohl in 1951 as the motion of bioparticles in response to the application of non-uniform electric fields.<sup>101</sup> If we consider a spherical dielectric particle in an electrolyte solution and apply an electric field, charges will accumulate at the interface between the particle and the surrounding electrolyte. In the case of a non-uniform electric field, the forces exerted on the sides of a polarizable particle are different thereby creating an imbalance in charge distribution which leads to the motion of the particle. It can experience positive DEP (pDEP) when the dipole's direction is towards the high strength electric field. In the case of negative DEP (nDEP), the situation is reversed, so the particle is repelled from the strong electric field (Fig. 3A). The dipole moment of the particle is a function of frequency, so the direction of the particle's passage depends on the frequency of the applied electric signal as well. Electrorotation of particles can be obtained in the microchip configuration with quadrupole electrodes. By the application of signals with different phases to the electrodes, a rotating electric field is induced (Fig. 3B).<sup>102</sup>

For a spherical particle with radius  $a$  suspended in a medium, the expression describing the time averaged DEP force acting on that particle is expressed as:

$$\langle F_{\text{DEP}} \rangle = \epsilon_m a^3 \text{Re} \left[ \frac{\tilde{\epsilon}_p - \tilde{\epsilon}_m}{\tilde{\epsilon}_p + 2\tilde{\epsilon}_m} \right] \nabla E^2$$

where  $\epsilon_m$  is the medium permittivity, and  $\nabla E^2$  is the gradient of the applied electric field.<sup>103</sup> The Clausius–Mossotti (CM) factor which describes the relation between the frequency of the applied electric field and the particle's polarizability is given by:

$$\tilde{f}_{\text{CM}} = \left( \frac{\tilde{\epsilon}_p - \tilde{\epsilon}_m}{\tilde{\epsilon}_p + 2\tilde{\epsilon}_m} \right)$$

where  $\tilde{\epsilon}_p$  and  $\tilde{\epsilon}_m$  are the complex permittivities of the particle and the medium, respectively. The crossover frequency is the frequency at which the particle changes its response from positive to negative DEP and inversely from nDEP to pDEP, the real part of the CM factor is equal to 0. Fig. 3C shows the case in which living and dead cells can be distinguished by the application of a signal with frequency near to the crossover frequency. In this instance living cells will follow the red line while dead cells the black line undergoing pDEP and weak nDEP or no DEP, respectively.

DEP has been applied for the manipulation of bioparticles with size varying between  $\sim 1$  and  $\sim 100 \mu\text{m}$ ,<sup>102</sup> however, the stimulation of smaller as well as bigger entities is possible. Two types of DEP microdevices can be distinguished: electrode DEP (eDEP) and insulator-based DEP (iDEP) in which the electrodes are protected by an insulating layer or a microstructure. The former allows for the creation of electric fields of high gradients using low voltages and thus enables the manipulation of micro scale particles. The latter generates electric fields of lower magnitude and has become applicable for the handling of nano scale (such as bacteria, viruses) and molecular size particles (such as biomolecules including DNA and proteins).<sup>104</sup>

### Optoelectronic tweezers

The principle of optoelectronic tweezers (OET) operation is based on the application of light onto a photosensitive layer ensuing a dielectrophoretic force in the illuminated area. Applied light reacts with a coating of hydrogenated amorphous silicon (a-Si:H) and combined with external bias creates gradients of the electric field.<sup>105</sup>

### Electrowetting on dielectric

Electrowetting on dielectric technology was developed in the 1990s,<sup>106</sup> although the phenomenon was already observed earlier. It originates from electrocapillarity studied and was described by Gabriel Lippmann around 1873–1875.<sup>107–109</sup> The expression describing EWOD actuation is the Young–Lippmann equation which demonstrates the relation of interfacial tensions between the three phases (Fig. 3D) and



Table 1 Dielectrophoresis in studies on gametes

No	Title and year	Objective	Materials	Methods	Main results	Species	Ref.
1	Enrichment of bovine X-sperm using microfluidic dielectrophoretic chip: a proof-of-concept study, 2020	Development of a MF-DEP chip for sperm sorting	ITO electrodes on glass, PDMS microchannel, silicone tubing (loading)	60 $\mu$ L sperm suspension DEP trapping: 4, 6, 8 V at 1–20 MHz	Strongest pDEP response: X-sperm at 8 V at 20 MHz, Y-sperm at 4 V at 1 MHz Quality of sperm decreased in low conductivity medium Double sorting at 4 V at 1 MHz, flow rate 0.1 $\mu$ l s <sup>-1</sup> significantly increased efficiency	Bovine	124
2	Distinct and independent dielectrophoretic behaviour of the head and tail of sperm and its potential for the safe sorting and isolation of rare spermatozoa, 2019	DEP chip for sorting of rare sperm cells	ITO and Cr/Au electrodes for simultaneous manipulation of the sperm head and tail Curved electrodes in the sorting chip PDMS microchannel Sigmacote coating	AC electric signal at 16–20 $V_{pp}$ at various frequencies	Independent crossover frequencies of the sperm head and tail Manipulation of the sperm using the tail, while distancing the head containing DNA from high electric field	Human	120
3	AC-electric-field induced parthenogenesis of mouse oocyte, 2018	Parthenogenetic activation of murine oocytes	ITO electrodes	Time dependence: 1–10 minutes with pDEP AC 10 V at 1 MHz Electrical field intensity: 1 min at 5–40 $V_{pp}$ at 1 MHz	Parthenogenetic activation successful: 80% of oocytes at 266.8 kV m <sup>-1</sup> , 50% at 133.4 kV m <sup>-1</sup>	Mouse	136
4	Towards microfluidic sperm refinement: impedance-based analysis and sorting of sperm cells, 2016	Development of a label-free, non-invasive MF chip for sperm analysis based on impedance measurements and sorting by DEP	Borofloat wafers, Ti/Pt electrodes, PerMX3020 foil, poly(L-lysine)-grafted-poly(ethylene glycol) (PLL-g-PEG, SuSoS) coating	Impedance measurements detection of cytoplasmic droplet DEP focusing: 3 V, 10 MHz	16/18 anomalous sperm positively identified	Boar	122
			2 chip designs: impedance detection (1) and impedance detection and DEP sorting (2)	DEP sorting: 2 V, 15 MHz	13/18 normal sperm cells positively identified Sorting of sperm cells and polystyrene beads by DEP based on impedance		
5	Dielectrophoresis of spermatozoa in viscoelastic medium, 2015	Investigation of sperm motility parameters for selection in ARTs	Theoretical analysis of sperm parameters under DEP force in a viscoelastic fluid	Oldroyd-B model	Velocities of spermatozoa presented as a function of the beating pattern and DEP force DEP force on sperm cells higher by an order of magnitude in a viscoelastic medium	Human model	123
6	AC electric field induced dipole-based on-chip 3D cell rotation, 2014	Development of the platform for 3D cell rotation with the use of AC electric fields	4 side micro-milled wall electrodes, 2 ITO bottom electrodes, mylar insulator, brass support for micro-milling, 25 × 25 mm cover slip as electrical and thermal barrier	10 $V_{pp}$ and 20 $V_{pp}$ at 10 kHz–10 MHz Yaw rotation: side wall electrodes with 90° phase shift, equal amplitudes	No effective difference in the rotation of ZP-intact and ZP-free oocytes Air bubble formation below 10 kHz No differences between clockwise and anti-clockwise rotation In-plane rotation: below 10 $V_{pp}$ no rotation	Bovine	118
				Pitch rolling rotation: 2 bottom electrodes (50° phase shift) and side wall electrodes (2 grounded, 2 floating), equal amplitudes	Out-of-plane rotation: at 10 V and 10 kHz, at above 15 V increased rates		



Table 1 (continued)

No	Title and year	Objective	Materials	Methods	Main results	Species	Ref.
7	Sperm cell manipulation employing dielectrophoresis, 2013	DEP chip for selection of immature and mature sperm cells	Microchannels with arrays of cylindrical insulators Borosilicate glass, Cr, photoresist	Application of DC potentials between 200 V and 1500 V for 30–60 seconds	Sperm trapping: 800 V: mature cells 1000 V: mature and little spermatogenic 1200 V: mature sperms exhibit stronger nDEP response, thus spermatogenic cells are separated Assessment of sperm cell viability under experimental conditions	Rat	121
8	Motile and non-motile sperm diagnostic manipulation using optoelectronic tweezers, 2010	OET response of human spermatozoa for separation of motile and non-motile sperm cells	PEG (poly(ethylene glycol)) coating Amorphous silicon electrode, 10 $\mu$ m silicon dioxide with melted onto the surface PEG-silane (Nektar). ITO electrode coated with PEG-silane (Nektar)	OET (40 mW cm <sup>-2</sup> ), 30 s Tryptan blue dye viability reference COMET assay (Trevigen, USA): DNA fragmentation	Dead sperm: weak nDEP or no response Live sperm: pDEP	Human	125
9	A noninvasive, motility independent, sperm sorting method and technology to identify and retrieve individual viable and nonviable nonmotile human sperm cells for ICSI	OET based microfluidic platform to distinguish between individual viable and nonviable nonmotile human sperm cells for ICSI	Glass with ITO electrodes, bottom plate coated with a 1 $\mu$ m film of amorphous silicon	Low dose: 10 $V_{pp}$ at 100 kHz, 80 mW cm <sup>-2</sup> , 20 s, high dose: 20 $V_{pp}$ at 100 kHz, 80 mW Velocity measurements at 9 $V_{pp}$ at 100 kHz, 40 mW cm <sup>-2</sup> Frequency: 100 kHz Up to 15 min OET assay Tryptan blue dye viability reference	No differences in DNA fragmentation between groups exposed to high and low dose of energy, isotonic and pure semen samples after OET Compatibility with unwashed semen samples	Human	126
10	A novel micropit device integrates automated cell positioning by dielectrophoresis and nuclear transfer by electrofusion, 2010	Automation of somatic cell nuclear transfer (SCNT) inside a MF device by positioning and electrofusion of cell couples	Coplanar Ti electrodes on borosilicate glass, SU-8 insulator (4 and 22 $\mu$ m thick) with micropits (diameters for 4 $\mu$ m thick: 10, 20, 30, 40 $\mu$ m; for 22 $\mu$ m thick: 20, 30, 40, 80 $\mu$ m)	DEP positioning: 3–6 $V_{rms}$ at 1 MHz Fusion DC pulses: 80 V–120 V	Fusion rates comparable with standard bovine NT: oocyte–oocyte (69%), oocyte–follicular cells (50%), oocyte–fibroblast (78%) Cell fusion of all cell types achieved between 110 and 120 V Cell lysis at voltages above 8 $V_{rms}$ upon positioning and at 160 V fusion Oocyte donor cell elongation and micropit structure imprinting on its surface at 6 $V_{rms}$ (4 $\mu$ m SU-8 with 40 $\mu$ m micropit)	Bovine	137



Table 2 Dielectrophoresis in embryo studies

No	Title and year	Objective	Materials	Methods	Main results	Species	Ref.
1	Using a dielectrophoretic microfluidic biochip enhanced fertilization <i>in vitro</i> , 2020	Investigation of fertilization rates at various sperm concentrations	ITO electrodes, PDMS microchannel	DEP entrapment: 10 $V_{pp}$ at 1 MHz for 1 min  Coculture in MF channel for 1 h Static droplet culture	Verification of the influence of HTF, KSOM + AA, DEP buffer on fertilization and blastocyst rates (no differences)  At total sperm count 3000 fertilization compatible with standard IVF group (17.2% +/- 7.5% vs. 14.5 +/- 7.5%)	Mouse	128
2	Automated embryo manipulation and rotation <i>via</i> robotic nDEP-tweezers, 2021	Non-invasive technique for manipulation of mouse embryos	PDMS cover, microchip mounted on a PCB, PVC petri dish on a motorized stage	Inverted chip placed 200 $\mu$ m above the embryo  DEP signal: 3 V  Frequency range 50–500 kHz Stage velocity: 4 $\mu$ m $s^{-1}$ or less	Effects of the chip height (100–250 $\mu$ m) and electric field strength (5–9 V) investigated  Speed of translation above 5 $\mu$ m $s^{-1}$ : embryo shape distortion  Relation of angular velocity and electric field strength (ER) Crossover frequency (ER): 150 kHz	Mouse	129
3	Dielectrophoretic microfluidic device for <i>in vitro</i> fertilization, 2018	MF-DEP platform to avoid unnecessary oocyte damage during IVF	ITO electrodes, PDMS microchannel	DEP entrapment: 10 $V_{pp}$ at 1 MHz, 30 s Droplets with gametes sorted with pneumatic valves KSOM/HTF culture	Focus on small sperm: oocyte ratio  Fertilization rates: 39.4% at 500 and 50.2% at 2000  Blastocyst rates: 33.3% at 500 and 25.1% at 2000	Mouse	130
4	Embryo formation from low sperm concentration by using dielectrophoretic force, 2015	MF-DEP microchip to imitate the mammalian oviduct during fertilization	PDMS microchannel, Cr and Au electrodes on a glass substrate	DEP entrapment: AC 10 $V_{pp}$ at 1 MHz  Flow rate: 0.1 $\mu$ l $min^{-1}$ Next, static droplet culture (until 8 cell stage)	Sperm concentration in oocyte vicinity increased from $1.5 \times 10^6$ sperm per ml (standard) to $\sim 6.0 \times 10^7$ per ml with trapping  Fertilization rate: 51.58%	Mouse	131
5	Preimplantation mouse embryo selection guided by light-induced dielectrophoresis, 2010	DEP for the selection of post-cleavage embryos for the purpose of embryo transfer	ITO glass, a-Si:H photosensitive layer, poly-ethylene glycol (PEG) coating (antiadhesive)	DEP of morphologically identical embryos cultured in M16 and KSOM+AA media 1-cell mouse embryo as an insulated core Blastocyst as an insulated shell  DEP signal: 20 $V_{pp}$ at 100 kHz	Determination of DEP response of preimplantation embryos at subsequent developmental stages  Comparison of M16 vs. KSOM + AA cultured embryos Contracted and granular embryos after the OET exposure cultured until blastocyst stages  Prolonged exposure to low conductivity medium: embryo death and decreased speed of OET  Suggestion: strongest nDEP of embryos points to the most matured ones	Mouse	127

Electrodes: ITO (indium tin oxide), amorphous silicon (a-Si), Cr (chromium), brass, Ti (titanium), Pt (platinum). Substrates: borosilicate glass, borofloat wafers, PCB (Printed Circuit Board). Coatings: photoresist, silicon dioxide, mylar, PerMX3020. Antifouling layers: PEG (polyethylene glycol), PEG-silane (Nektar), PLL-g-PEG (poly(L-lysine)-grafted-poly(ethylene glycol), SuSoS), Sigmacote (Sigma Aldrich). Walls/dish: PDMS (polydimethylsiloxane), PVC (polyvinylchloride).

the change in surface energy under the influence of an electric field. Electrocapillarity refers to the capillary rise of the liquid under the influence of the electric potential.<sup>83</sup> In conventional electrowetting (EW), as voltage is applied, an electric double layer (EDL) is created between the solid and

the electrolyte. In electrowetting on dielectric, as the name suggests, a dielectric layer is incorporated between the electrode and the liquid. In both cases, the interfacial energy is modulated due to a charge imbalance in the EDL (EW), or the insulator (EWOD) caused by the external



Table 3 Electrowetting on dielectric in gametes and embryo manipulation

No	Title and year	Objective	Materials	Methods	Main results	Species	Ref.
1	Digital microfluidic dynamic culture of mammalian embryos on an electrowetting on dielectric (EWOD) chip, 2015	Development of a DMF chip to mimic the fallopian tube and embryo travel <i>in vivo</i>	ITO electrodes, silicon nitride and spun on glass, Teflon	Single embryo in 1 $\mu$ l droplet 4 $\mu$ l oil overlay	Comparable blastocyst rates of dynamic EWOD and static culture (88.9 $\pm$ 4.2% vs. 92.1 $\pm$ 10.8%) Higher rates of hatching blastocyst on EWOD chip than in static culture (50 $\pm$ 9.8% vs. 21.2 $\pm$ 5.5%) EWOD manipulation: 60–68.5 $V_{rms}$ at 500 Hz	Mouse	139
2	Fertilization of mouse gametes <i>in vitro</i> using a digital microfluidic system, 2015	Dynamic fertilization and culture of mouse embryos on a DMF chip	ITO electrodes, silicon nitride and spun on glass, Teflon, PDMS to create the oil bath	5 $\mu$ l droplets containing sperm cells (various concentrations) and cohorts of oocytes (10) EWOD manipulation: 60 $V_{rms}$ at 500 Hz	10/19 viable pups after embryo transfer into 3 recipients Biocompatibility tested with static culture of 2-cell embryos	Mouse	138
3	Digital microfluidic processing of mammalian embryos for vitrification, 2014	Execution of the process of embryo vitrification on chip	Cr and ITO electrodes, polyimide C, Teflon	200 nl droplet containing embryo mixed with cryoprotectant droplets EWOD manipulation: 55–75 $V_{rms}$ at 15 kHz	Fertilization rate correlated with the amount of sperm cells in the sperm droplet The developmental rates conversely correlated with the sperm concentration on the DMF chip Minimized timing and washing steps	Mouse embryos	142
4	Transport of live yeast and zebrafish embryo on a droplet (“digital”) microfluidic platform, 2009	Transport of live yeast and a zebrafish embryo on a DMF transport	Au electrodes, ITO top electrode, polyimide C or silicon dioxide, Teflon	5 $\mu$ m live yeast in 500 nl droplets EWOD manipulation: 80 $V_{rms}$ at 7 kHz 500 $\mu$ m zebrafish embryo in 20 $\mu$ l droplets EWOD manipulation: 95–105 $V_{rms}$ at 8 kHz	Exclusion of manual pipetting Comparable survival rates DMF vs. manual (77% vs. 73%) Comparable developmental rates DMF vs. manual (90% vs. 91%) On chip manipulation of viable yeast Dechorionation of a 500 $\mu$ m zebrafish embryo Culture of an embryo which experienced electrolysis during on chip operation	Live yeast, zebrafish embryo	140

electric field. Consequently, the apparent contact angle  $\theta$  of the liquid droplet on a solid surface is altered (Fig. 3E). The insulating coating plays a significant role in EWOD since the required voltage to induce surface wetting depends on its thickness and dielectric properties. Additionally, the most common practice includes coating of the insulator with a hydrophobic material (low surface energy) to achieve the highest possible initial contact angle with the aqueous conductive droplet.

The change of the contact angle as a function of the applied voltage (Young–Lippmann equation) is given by:

$$\cos \theta' = \cos \theta + \frac{1}{2} \frac{cV^2}{\gamma_{lv}}$$

where  $\theta'$  and  $\theta$  are the potentiated and initial contact angles of a liquid droplet on a solid surface, respectively,  $V$  is the applied voltage,  $\gamma_{lv}$  is the interfacial tension between the liquid and vapour and  $c$  is the capacitance of the insulator.

Digital microfluidics allows for rapid transport, merging and splitting of pico- to microdroplets ( $10^{-12}$ – $10^{-6}$  l).<sup>110–113</sup> Droplet motion is achieved on an array of electrodes. Two



Table 4 Electrowetting on dielectric in embryo assessment

No	Title and year	Objective	Materials	Methods	Main results	Species	Ref.
1	Simultaneous detection of two growth factors from human single embryo culture medium by bead based digital microfluidic chip, 2020	Detection of IL-1 $\beta$ and TNF- $\alpha$ from spent culture media after single human embryo culture	ITO electrodes, SU-8/Al <sub>2</sub> O <sub>3</sub> , Cytop, magnetic beads conjugated with antibodies specific for the biomarkers of interest	Fluorescence detection of both factors from 32.5 nL, 325 nL and 520 nL droplets	Concentration of IL-1 $\beta$ in blastocyst medium (BM) higher than in cleavage medium (CM), no change in the concentration of TNF- $\alpha$ between CM and BM	Culture media from human embryo culture	146
2	A medical innovation: a new and improved method of DNA extraction with electrowetting-on-dielectric of genetic testing in-vitro fertilization (IVF), 2020	Application of EWOD chip for extraction of cell free DNA from mouse embryo culture medium	ITO electrodes, silicon dioxide or SU-8, Cytop, magnetic beads	100 nL droplets  EWOD manipulation: 50–70 V <sub>rms</sub> at 2 kHz	Cf-DNA extraction protocol adapted) followed by qPCR analysis  Not all operations achieved on the chip (buffer incompatibility)  Chip cleaning procedure proposed  On-chip cf-DNA extraction higher than the standard procedure (18% vs. 7%)	Culture media from mouse embryo culture	145
3	Extraction of cell free DNA from an embryo culture medium using micro scale bioreagents on EWOD, 2020	Application of EWOD chip for the extraction of cell free DNA from mouse embryo culture medium	DropBot model DB3-120 from Sci-bots with magnetic beads	1–1.8 $\mu$ L droplets  EWOD manipulation: 80–100 V <sub>pp</sub> (depending on the buffer), 2 kHz	Entire extraction performed on chip followed by qPCR analysis  On-chip cf-DNA extraction higher than the standard procedure (23% vs. 14.8%)  Chip cleaning procedure proposed	Culture media from mouse embryo culture	144

Electrodes: ITO (indium tin oxide), Cr (chromium), Au (gold). Insulating layers: SU-8/Al<sub>2</sub>O<sub>3</sub>, silicon dioxide, SU-8, silicon nitride and spun on glass (SOG), parylene C. Hydrophobic coatings: Cytop, Teflon. Substrates: glass, PCB (printed circuit board). Walls: PDMS (polydimethylsiloxane). Additional: magnetic beads, magnetic beads conjugated with antibodies.

chip configurations exist: the droplet is either sandwiched between or placed on top of the electrode pairs. By sequential charging and discharging of the electrode pairs, the droplet movement is induced and as a result, the liquid is attracted towards the actuated electrode (Fig. 3F and G).

## DEP and ER in ARTs

### Gamete and embryo handling: positioning, selection, sorting

The size and shape of gametes and early embryos make them perfect candidates for on-chip manipulation by means of dielectrophoresis and electrorotation. Based on the study performed on 103 samples collected from men undergoing semen analysis for the assessment of fertility, the mean total sperm length was 48  $\mu$ m, of which 4.31  $\mu$ m, 2.04  $\mu$ m and 43.76  $\mu$ m were the head, the midpiece and the sperm tail, respectively.<sup>114</sup> Although human blastocysts may be too big for DEP stimulation ( $\sim$ 194  $\mu$ m on day 5),<sup>115</sup> mature oocytes (110–120  $\mu$ m)<sup>116</sup> and immature oocytes (100–110  $\mu$ m), which can be collected and successfully matured in *in vitro* setting,<sup>116,117</sup> are applicable for on chip handling by DEP force. Moreover, bovine oocytes ( $\sim$ 120  $\mu$ m), which more closely resemble

the human egg in size,<sup>31</sup> were rotated using electric fields.<sup>118</sup> Murine oocytes (80  $\mu$ m)<sup>31</sup> as well as blastocysts (100–110  $\mu$ m)<sup>119</sup> can serve as promising tools for the investigation of the effects of the application of electric potential on the *in vitro* development of human embryos. Note that the above-mentioned size of oocytes and embryos provided in brackets is the diameter. The DEP force exerted on mammalian gametes and embryos can be calculated using models of a homogenous or single-shelled sphere, or an ellipsoid. Below, a summary of the work on DEP microelectromechanical systems published in the last decade divided by the cells handled including sperm, oocytes and embryos is provided. Additionally, significant information about the chips and protocol development is collected in chronological order in Tables 1 and 2.

### Sperm

Shuchat *et al.* fabricated a microsystem to sort and investigate the properties of human spermatozoa.<sup>120</sup> The study revealed that both the head and the tail have intrinsic dielectric features and thus were modelled separately, as a



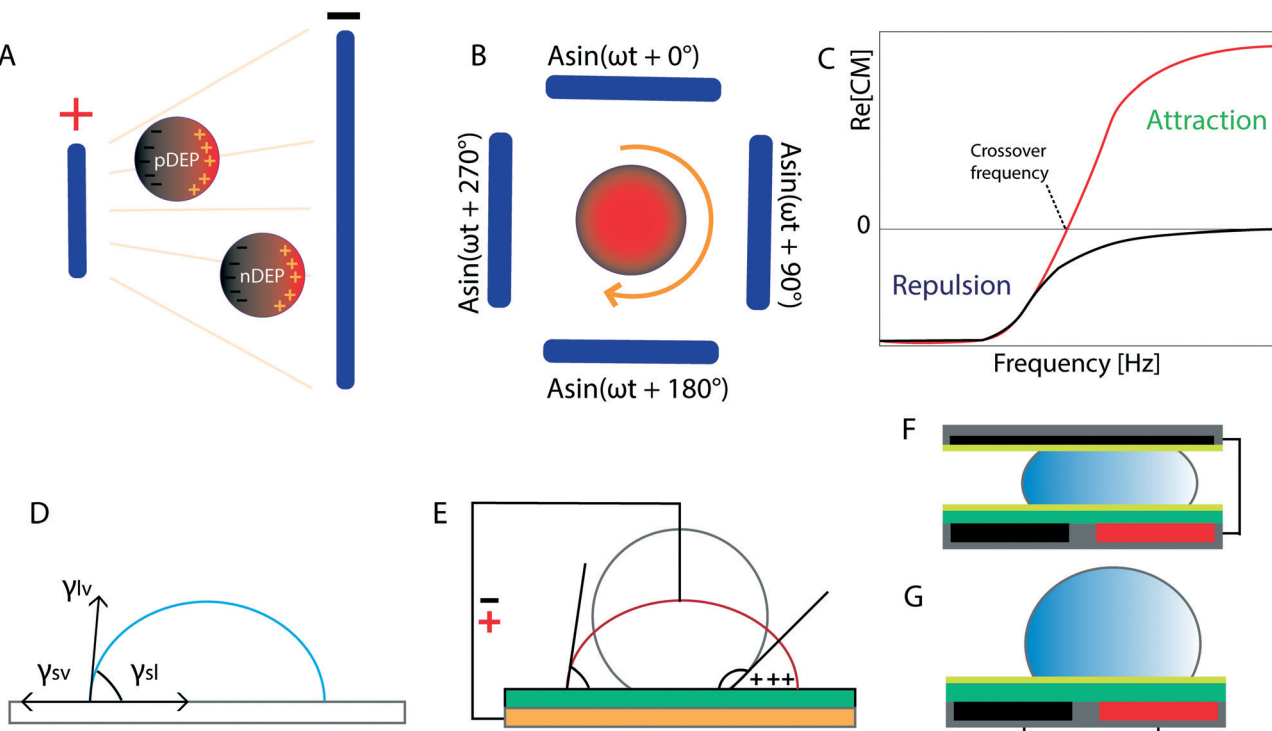


**Fig. 3** Electric fields in lab-on-a-chip microfabrication: dielectrophoresis, electrorotation and electrowetting on dielectric. (A) Dielectric spherical particle responses to the non-uniform electric field: positive and negative DEP. Adapted from ref. 103 with permission from Springer. (B) Quadrupole electrodes with signals with  $90^\circ$  phase shift to induce electrorotation. Adapted from ref. 103 with permission from Springer. (C) DEP response of polarizable particles ( $\epsilon_p > \epsilon_m$ ) to the applied electric field. Crossover frequency: relation of  $\text{Re}[\text{CM}]$  with the frequency of the applied signal. Reproduced from ref. 86 with permission from MDPI (CC BY 4.0). (D) Droplet equilibrium. (E) EWOD representation in a sessile droplet experiment. (F) Closed and (G) open configuration of EWOD. Figures D–G were adapted from ref. 83 with permission from Springer.

sphere and an ellipsoid, respectively (Fig. 4A–E). Their crossover frequencies were evaluated experimentally. It was found that at low frequencies, both the head and tail exhibited nDEP while at high frequencies, a positive DEP response is achieved. In the middle range, however, the tail underwent pDEP while the head was exposed to nDEP. The proposed sorting microdevice utilized the pDEP of the tail, while distancing the head, which contains the genetic material, away from the high electric fields.

An insulator DEP (iDEP) based microdevice was fabricated by Rosales-Cruzaley *et al.* for the separation of mature and immature sperm.<sup>121</sup> Differences in morphologies among spermatogenic (immature) and mature sperm give rise to various DEP responses when subjected to an electric field. Successful trapping and sorting at 1200 V was based on the distinguishably stronger nDEP of mature sperm cells. Additionally, the cell viability was evaluated and found to decrease upon increasing the exposure time and the magnitude of the electric field. Nevertheless, 75% of cells remained viable upon treatment for 60 s at 800 V.

An impedance based sperm analysis microsystem was developed for the detection of a cytoplasmic droplet on the flagellum of the sperm, an anomaly arising during spermatogenesis.<sup>122</sup> De Wagenaar *et al.* utilized different impedometric characteristics of morphologically distinct normal and anomalous spermatozoa which passed through

the microchannel. Next, in a proof-of-concept experiment, sperm cells and polystyrene beads were sorted by DEP based on impedance measurements (Fig. 4F and G).

J. Koh and Marcos performed a theoretical analysis of a sperm cell in a viscoelastic medium subjected to DEP force to predict the sorting efficiency in an *in vivo*-like microenvironment.<sup>123</sup> Motility parameters such as morphology, dimensions, velocity and the frequency of the flagellum beating were analysed using an Oldroyd-B model. A relation between the spermatozoa velocities and the beating pattern of the flagellum and DEP was revealed. Interestingly, the DEP force exerted on the sperm was found to be higher by an order of magnitude under the proposed conditions which can be useful in the development of a novel, more biomimetic (D)MF device. Employing DEP as a technique for gender sperm sorting was suggested which was later executed experimentally.<sup>124</sup>

T. Wongtawan *et al.* developed a microchip for categorization of X- and Y-sperm. It was suggested that the differences in the composition of cell membrane proteins and electrokinetic potential resulted in the different DEP response.<sup>124</sup> The study showed that Y-sperm was more sensitive to frequency changes, while X-sperm to changes in voltage. However, different bull donors, buffers, electric signals and fluid flow rates affected the grouping process. Adaptation of the chip for double sorting at 4 V at 1 MHz,

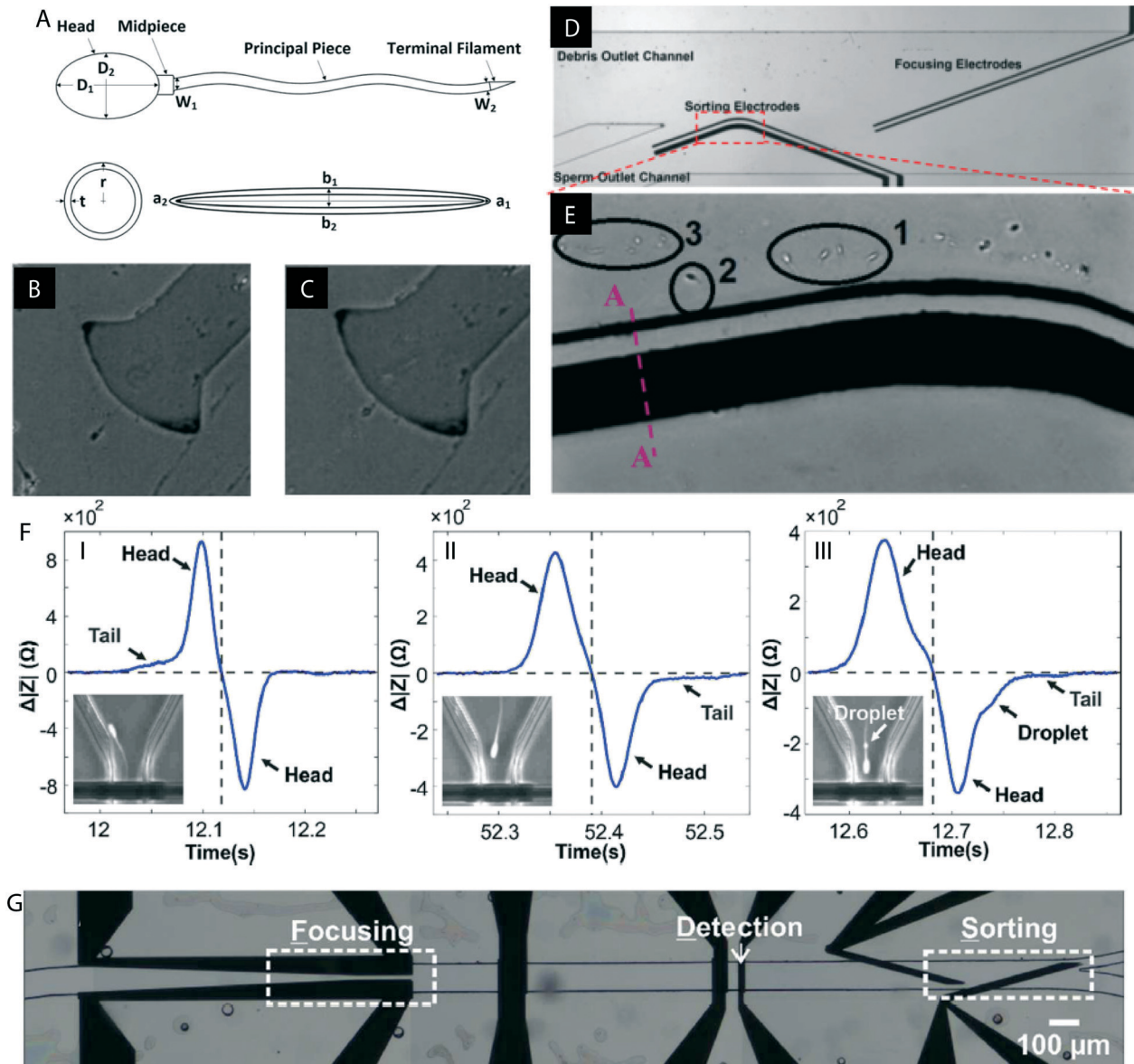


**Fig. 4** Examples of DEP microdevices for sperm processing. (A) Human spermatozoon with separately modelled spherical head and ellipsoidal tail. (B and C) Distinct responses of the tail and the head under the influence of the applied electric field (medium conductivity  $110 \text{ mS m}^{-1}$ ). (B) pDEP of the tail and strong nDEP of the head at  $300 \text{ kHz}$ , (C) pDEP of the tail and weak nDEP of the head at  $1500 \text{ kHz}$ . (D and E) Example of the DEP chip for sperm sorting and focusing. (E) Live sperm cells (1 & 2) trapped by DEP of the tail while debris (3) flows with the fluid. Figures A–E were republished with permission of John Wiley & Sons Inc from ref. 120; permission conveyed through Copyright Clearance Center, Inc. (F) Detection of the cytoplasmic droplet on the sperm tail based on impedance measurements. (G) Proof of concept experiment: DEP sorting of polystyrene beads and spermatozoa based on the different impedometric characteristics. Figures F and G were reproduced from ref. 122 with permission from the Royal Society of Chemistry.

flow rate  $0.1 \mu\text{l s}^{-1}$ , resulted in significant reduction of the Y-sperm in the sorted sperm, thereby enhancing the chip efficiency.

Optoelectronic tweezers proved useful for spermatozoa sorting and two examples of such applications exist. Ohta *et al.* developed OET for the manipulation of motile and non-motile human spermatozoa.<sup>125</sup> Dead sperm cells could be distinguished by the lack of or a very weak nDEP response, while living sperms underwent pDEP. Additionally, the assessment of DNA damage among sperms exposed to the

independent components of the OET platform was performed (low-conductivity medium, passage of cells through the microfluidic chip, dose of OET) and no differences between the groups were found. Moreover, the device proved compatible with the unwashed semen samples.

An OET assay for sorting of viable non-motile *vs.* non-viable non-motile human spermatozoa was proposed by Garcia *et al.*<sup>126</sup> Non-motile viable sperm cells were attracted to the induced electric field, whereas non-viable ones were repelled from it or exhibited no response. The results



indicated that the motility independent assay is comparable with the standard Trypan Blue staining reference. This microsystem was proposed as a tool for sperm selection for ICSI when motility is not present or hardly detectable.

### Oocyte and embryo

J. K. Valley *et al.* proposed optoelectronic tweezers for the selection of preimplantation mouse embryos.<sup>127</sup> The DEP response of 1-cell, 2-cell, 4- to 16-cell until morula, early blastocysts and late blastocysts was evaluated. Morphologically identical embryos cultured in M16 or KSOM + AA were used in the study as the former suboptimally sustains murine early embryo development *in vitro*. It was found that both M16 and KSOM + AA, early embryos until the morula stage underwent pDEP at 20 V<sub>pp</sub> at 100 kHz, while early blastocysts were repulsed from the light pattern exhibiting nDEP response (Fig. 5A–C). Some embryos appeared contracted and granular after OET treatment. However, despite visible changes in their structure, they were successfully cultured until blastocysts and thus altered morphology was linked to the low conductivity DEP medium. Based on the results, it was suggested that among morphologically undistinguishable mouse embryos, the one exhibiting the strongest nDEP response is the most matured.

K. Huang *et al.* proposed a nDEP microdevice with a proportional integral derivative (PID) controller for precise manipulation of mouse embryos.<sup>128</sup> The inverted microsystem consisting of quadrupole electrodes mounted on a motorized platform was utilized to transport, position and rotate murine embryos. Effects of chip height and input voltages were investigated and a set of parameters for safe handling was established. Additionally, it was found that the increasing speed of translation, which was achieved by the actuation of two pairs of oppositely situated electrodes with signals of the same amplitude with a 90° phase shift, would result in the distorted shape of manipulated cells. Electrorotation was obtained by potential application to four electrodes with equal amplitude and 90° phase shift, upon which a relation between the strength of the applied electric field and the angular velocity was established.

Benhal *et al.* fabricated a microdevice for the 3D rotation of zona pellucida-intact (ZP-intact) and zona pellucida-free (ZP-free) bovine oocytes.<sup>118</sup> The chip consisting of four side walls and two bottom electrodes was designed to enable the two-axial rotation of mammalian eggs (Fig. 5D–H). Vertical electrodes were used for the yaw rotation whereas bottom electrodes in combination with side wall electrodes allowed for the pitch rolling rotation. The influence of the frequency, amplitude and medium conductivity on the motion of bovine ova was evaluated and compelling observations were made.

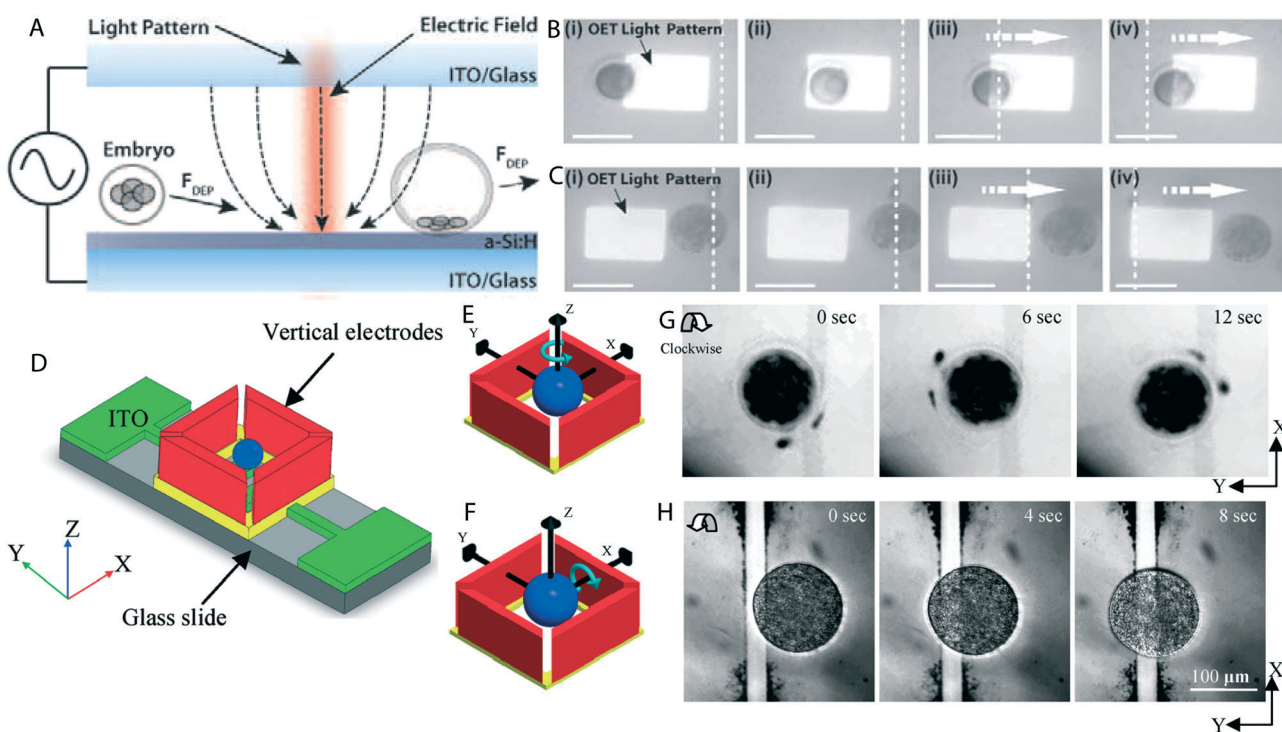


**Fig. 5** Examples of DEP microdevices for oocyte and embryo processing. (A) Light-induced DEP of a developing mouse embryo. (B) Manipulation of 1-cell embryo with pDEP (attraction towards the light pattern). (C) Embryo at the blastocyst stage undergoing nDEP (repulsion from the light pattern). Scale bars represent 100 microns. Figures A–C were reproduced from ref. 127 with permission from PLOS ONE. (D) Configuration of the chip for 3D rotation of bovine oocytes. Schematic representation of (E) in-plane and (F) out-of-plane rotation of a spherical particle subjected to the electric field. (G) Clockwise in-plane rotation of a ZP-free oocyte. (H) Clockwise rolling rotation of a lysed oocyte. Figures D–H were reproduced from ref. 118 with permission from the Royal Society of Chemistry.



Firstly, the oocytes followed the Gaussian distribution characteristic in the range of applied frequencies, *i.e.* at low or high frequencies they did not undergo electrorotation, but in the middle range a peak frequency was distinguished at which they rotated in the fastest manner. Next, the increase in the amplitude of the applied potential resulted in the faster rotation and a relation between the frequency and amplitude of the applied signal was found. At the frequency of 1 MHz bovine ova reached the peak rotation at 20 V, while at 2 MHz the peak was found at 10 V. Lastly, no differences in the rotation rates were observed between the media used which differed in conductivity.

### DEP in other studies: IVF, cloning

**IVF.** H.-Y. Huang *et al.* proposed three microchips utilizing positive dielectrophoresis for the fertilization of murine oocytes *in vitro*.<sup>129–131</sup> In all studies, an AC signal of 10 V<sub>pp</sub> at 1 MHz was used for the entrapment and co-incubation of gametes. Various microchannel configurations were created to mimic the conditions in the fallopian tubes at the time of fertilization *in vivo* and to avoid the unnecessary handling of gametes as is the case for traditional IVF. In all cases, the pDEP trapping of gametes resulted in higher fertilization rates at low sperm-oocyte ratios and increased sperm cell concentration in the vicinity of the murine ovum. The calculated transmembrane potential in ref. 129 for the oocyte and sperm under pDEP trapping conditions was 8.47 mV and 8.95 mV, respectively (electroporation of the cell membrane occurs at 100 mV and higher). Thus, the DEP manipulation was considered safe for the cells. This technique was proposed as a non-invasive alternative for ICSI, especially for patients with oligoospermia, which yet allows for natural fertilization to occur *in vitro*.

**Cloning.** Parthenogenesis is a form of asexual reproduction in which the oocyte is activated in the absence of a sperm,<sup>16</sup> an important aspect in cloning studies. In mammals, it can be induced by exposure to chemical substances which can affect the intracellular calcium oscillation pattern, such as ethanol, strontium chloride and others.<sup>132–134</sup> It has been shown recently that parthenogenesis can be affected by numerous aspects in mouse oocytes.<sup>135</sup> H.-Y. Huang *et al.* developed a DEP microchip for parthenogenetic activation of mouse eggs.<sup>136</sup> The rates of activation were independent of the time of DEP exposure varying between 1 and 10 minutes at 10 V and 1 MHz. However, a dependence on the strength of the applied electric field was found. 50% and 80% of oocytes were successfully activated by the application of high intensity electric fields of 133.4 kV m<sup>−1</sup> and 266.8 kV m<sup>−1</sup>, respectively. More than 80% of ova remained viable for both electric field strengths.

Electrofusion is a technology that involves the production of a cell with new genetic material and has been applied in cloning, regenerative medicine, plant hybridization and somatic cell nuclear transfer (SCNT). Clow *et al.* developed a

DEP microdevice with micropit structures of various diameters for the positioning and electrofusion of bovine cell couplets.<sup>137</sup> By the application of AC signals for cell positioning and DC fusion pulses, cells were immobilized at the desired spot(s) on the insulating film and allowed for successful nuclear transfer (NT). Bovine oocyte–oocyte (69%), oocyte–follicular cell (50%) and oocyte–fibroblast (78%) couplets were fused at rates proportional to the standard bovine cell NT. Cell lysis occurred at voltages exceeding 8 V<sub>rms</sub> upon cell positioning and at higher rates at 160 V DC pulse.

### EWOD in ARTs

Although electrowetting on dielectric technology has already entered the field of on-chip manipulation of reproductive cells, it is more extensively utilized as a chemical reactor for (bio)fluid processing. This technology proved suitable for the manipulation of culture medium microdroplets with gametes and embryos during the dynamic automated culture. Furthermore, EWOD can be used for the processing of spent embryo culture medium, an important step in the assessment of the embryo developmental competence based on the analysis of its secretome. Information about the chips and protocol development for the *in vitro* manipulation of gametes and embryos as well as analysis of the culture medium are collected in chronological order in Tables 3 and 4.

### On chip handling of gametes and embryos: IVF, IVC, vitrification

H.-Y. Huang *et al.* fabricated an open EWOD chip for the fertilization of mouse oocytes by merging 5 µl droplets containing sperm cells (at various concentrations) and ten ova followed by dynamic culture.<sup>138</sup> Droplets were translated and merged with 60 V<sub>rms</sub> at 500 Hz. The results showed that the fertilization rates correlated with the amount of sperm cells in the sperm droplet, *i.e.* the higher the concentration of sperm, the higher the percentage of fertilized oocytes. The developmental rates, however, were found to conversely correlate with the sperm concentration, suggesting that the excess of sperm cells remaining in the culture medium droplet affects the early embryo development. In the open device configuration, splitting of the droplet is so far impossible to achieve. Thus, the inhibited embryo development was associated with medium instability (such as imbalance in ion concentration, pH) caused by the presence of the spermatozoa.

The same group proposed a similar EWOD platform for the dynamic culture of mouse embryos.<sup>139</sup> Single 2-cell mouse embryos were dynamically cultured in 1 µl droplets of culture medium covered by 4 µl of oil on the chip with coplanar electrodes and in a closed configuration (Fig. 6A and B). Droplet motion was achieved by the application of 60–68.5 V<sub>rms</sub> at 500 Hz. Generally, the blastocyst rates of the dynamically actuated embryos were



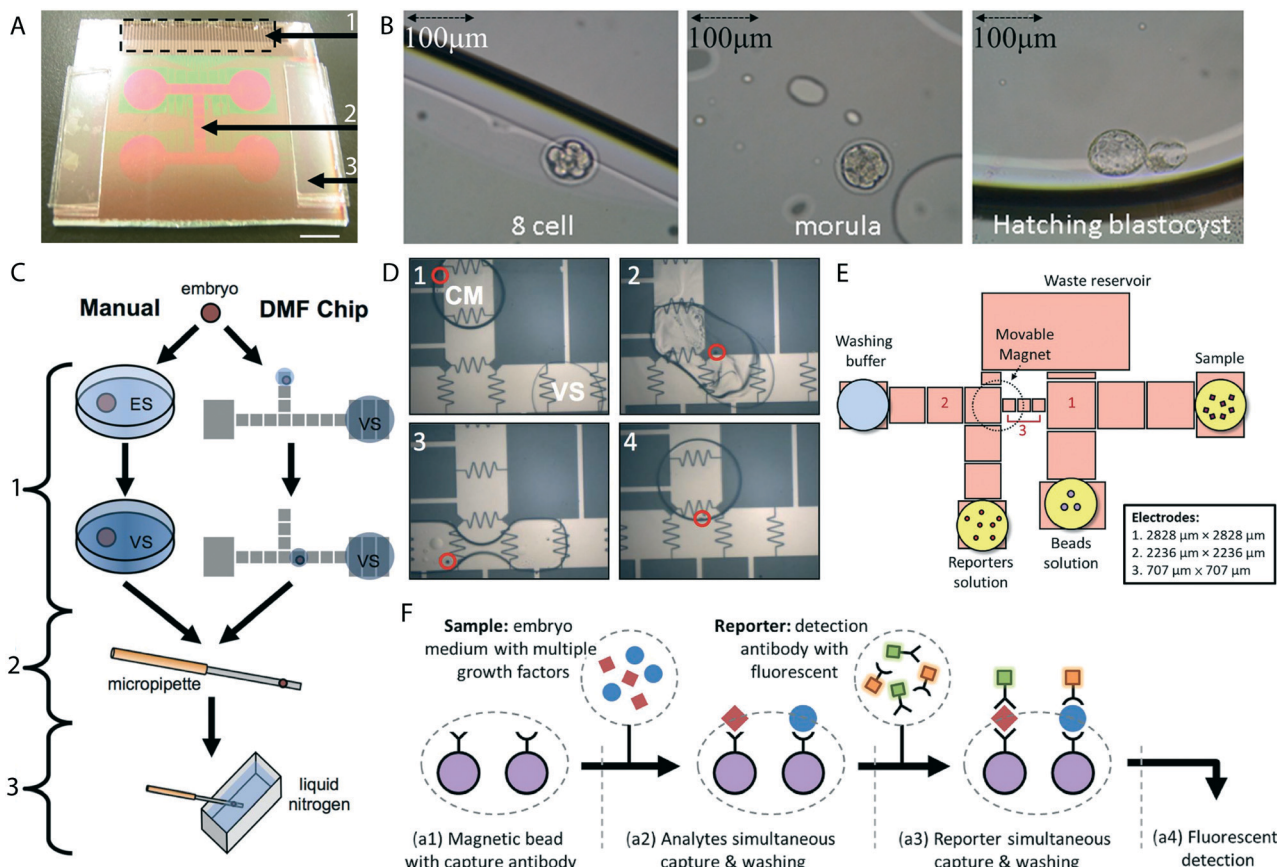


**Fig. 6** EWOD microsystems for processing and assessment of embryos. (A) EWOD chip for the dynamic culture of mammalian embryos. 1) Contact pad, 2) microfluidic channel (electrodes), 3) spacer (260  $\mu\text{m}$ ). Scale bar 6 mm. (B) Mouse embryo at subsequent developmental stages cultured on the digital microfluidic chip. Figures A and B were reproduced from ref. 139 with permission from PLOS ONE. (C) Standard and on-chip protocol for vitrification of mouse embryos. ES-equilibrium solution, VS- vitrification solution. 1) Cryoprotectant stage, 2) extraction stage, 3) freezing stage. (D) On-chip mixing of droplets of culture medium (CM) containing a mouse embryo with droplets of vitrification solution (VS). Figures C and D were reproduced from ref. 142 with permission from PLOS ONE. (E) Pattern of the electrodes for simultaneous on-chip detection of IL-1 $\beta$  and TNF- $\alpha$ . (F) Schematic representation of simultaneous detection of two single-embryo growth factors (SEGf) from culture medium. Figures E and F were reprinted from ref. 146 with permission from Elsevier.

comparable with the ones cultured statically. The dynamic group, however, showed a significant increase in the percentage of hatching blastocysts. Additionally, embryos cultured on the chip (19) were transferred to three recipient mice and resulted in the births of viable pups (10/19) among all three of them.

Son *et al.* developed an EWOD chip for the automated handling of live yeast and zebrafish embryos, which, to the best of our knowledge, was the first attempt of embryo manipulation by EWOD.<sup>140</sup> 5  $\mu\text{m}$  yeast cells were suspended in 0.5  $\mu\text{l}$  droplets and successfully transported with 80  $V_{\text{rms}}$  at 7 kHz with no viable yeast left on the chip after motion. A 500  $\mu\text{m}$  diameter zebrafish embryo was handled in a 20  $\mu\text{l}$  droplet with voltages ranging from 95  $V_{\text{rms}}$  to 105  $V_{\text{rms}}$ . Additionally, embryo dechorionation was achieved by mixing the droplets containing the embryo and the digestive agent. The process of chorion removal, an envelope surrounding the embryo, is common in ecotoxicological testing for better visualization, exposure to chemicals and cell handling (microinjection, transfection).<sup>141</sup> On-chip dechorionation was

proposed as an alternative to the standard, manual procedure. Interestingly, one of the zebrafish embryos was exposed to electrolysis after which it was removed from the platform and cultured in a fresh water tank. Despite the occurrence of electrolysis, the embryo successfully developed further.

Pyne *et al.* developed an EWOD chip for the processing of mammalian embryos for vitrification, an “ice-free” rapid cryopreservation technique in which cells are mixed with cryoprotectants.<sup>142</sup> This method avoids the formation of intracellular ice upon rapid freezing. This preferred approach in gamete and embryo cryopreservation became dominant over the fresh donor embryo transfer in recent years.<sup>143</sup> In the study, the adapted human and mouse embryo vitrification protocols were translated for the on-chip manipulation of a single murine embryo (Fig. 6C and D). Droplets containing the embryo and cryoprotective reagents were mixed, split and transported with 55–75  $V_{\text{rms}}$  at 15 kHz. Survival and developmental rates were assessed by morphological grading before and after freezing as well as

after thawing and culture of 8-cell stage embryos for 24 h. Serum-free culture medium was used to avoid chip surface contamination. The results of the on-chip vitrification were comparable with the standard, manual protocols.

### Embryo assessment

A promising field of application of digital microfluidics is the isolation of developmentally significant biomarkers from spent cell culture medium. EWOD chips are under evaluation as instruments in various “omics”, fields of study such as genomics, proteomics, transcriptomics, cellomics and metabolomics,<sup>92</sup> the main purpose being the characterization of molecules that are involved in various cellular processes to better understand their function.

Two procedures of cell-free DNA (*cf*-DNA) extraction with DMF from spent mouse embryo culture medium were proposed recently. Alias *et al.* used the commercially available platform DropBot (model DB120 from Sci-bots, <https://shop.sci-bots.com/product/dropbot-db3-120-kit/>) with magnetic beads for the isolation of *cf*-DNA from culture medium collected at days 2.5 (4-cell stage) and 3.5 of culture (8-cell until morula stages). Depending on the buffer used in the protocol, the applied signals varied between 80  $V_{pp}$  and 100  $V_{pp}$  at 2 kHz for the transport of 1–1.8  $\mu$ l droplets. A higher percentage of *cf*-DNA was extracted from the EWOD chip as compared with the conventional method (23% *vs.* 14.8%, respectively).<sup>144</sup> Another example is the EWOD chip with magnetic beads developed by Chiang *et al.*<sup>145</sup> The DNA extraction protocol was previously adapted to the requirements of the microdevice. The performance of the microsystem was evaluated using two different dielectric layers, which was shown to affect the performance. The operating voltages ranged from 50  $V_{rms}$  to 70  $V_{rms}$  at 2 kHz for 100 nl droplets. The on-chip *cf*-DNA isolation resulted in higher percentages as compared to the standard protocol (18% *vs.* 7%). However, not all of the extraction operations were achievable on the chip due to the incompatibility of some reagents with the proposed EWOD platform. In both cases, a cleaning procedure was proposed allowing for chip reusability.

Lee *et al.* fabricated a bead-based microchip for the simultaneous isolation of interleukin  $\beta$  (IL-1 $\beta$ ) and tumour necrosis factor  $\alpha$  (TNF- $\alpha$ ).<sup>146</sup> IL-1 $\beta$  is a cytokine secreted by growing mammalian embryos *in vitro* at later developmental stages (8-cell to blastocyst) and a correlation between its concentrations and the implantation rates was found.<sup>147</sup> Thus, it could be considered a potential biomarker for embryo implantation. TNF- $\alpha$  was found to be involved in maintaining the balance between the embryotoxic and embryotrophic cytokines during early embryo development, and additionally affects the hormonal balance during gestation as well as influences the reproductive function in males.<sup>148</sup> Both molecules were fluorescently detected with the use of magnetic beads conjugated with a specific antibody for each cytokine. 32.5, 325 and 520 nl droplets of

spent human embryo culture medium and reagents were manipulated on the chip (Fig. 6E and F). Culture media from day 3 and days 5–6, cleavage medium (CM) and blastocyst medium (BM), respectively, were collected with no interference with the IVC protocol. It was shown that concentrations of IL-1 $\beta$  differed between the cleavage and blastocyst media while no changes in the levels of TNF- $\alpha$  were found. Interestingly, significant differences between the concentrations of growth factors can be found between the embryos collected from the same patient which calls for further validation of this technique exploiting an increased number of test samples. The extraction of these as well as other biomarkers could potentially serve as a non-invasive tool for the assessment of early embryonic development as well as facilitate the prediction of the implantation competence.

## Discussion: benefits and challenges

### Benefits of the application of electric fields in ARTs

The continuously growing field of application of DEP and EWOD biochips covers at present multiple operations which supersede or at least optimize the current techniques used in assisted reproduction. Direct manipulation of gametes and embryos ranges from positioning and entrapment, detection of anomalies, separation of living and dead, mature and immature, viable motile and viable non-motile sperm cells through the 3D rotation of oocytes, electrically induced parthenogenesis and electrofusion towards the selection of embryos at various developmental stages. Morphological grading of embryonic development *in vitro* could be supported by more advanced technologies for the *in vitro* assessment and selection of gametes and embryos for IVF. Moreover, IVF and IVC were successfully achieved on DEP and EWOD chips. Indirect application of EWOD microdevices for the isolation of cell-free DNA and other potentially valuable biomarkers of early embryonic development, and implantation from a single mammalian embryo during culture already outperforms the existing procedures. Importantly, it allows for the analysis on a single embryo level, thus far unachievable due to the constraints of standard approaches such as the requirement for large sample volumes (520 nl sample on EWOD platform *vs.* minimum 50  $\mu$ l required for enzyme-linked immunosorbent assay, ELISA).<sup>146</sup> Until now, DEP and EWOD proved to be promising tools towards the improvement of IVF laboratory procedures. The advantages of microdevices utilizing DEP and EWOD in reproductive studies are listed in Table 5.

### Challenges for biochips for ARTs utilizing electric fields

Although automated miniaturized chips for the *in vitro* manipulation of cells and fluids possess numerous advantages, several challenges need to be overcome. When designing a microdevice utilizing electric fields for a biological application, one needs to take into consideration both the constraints stemming from the microfabrication



Table 5 Advantages of electric fields in assisted reproductive technologies

Method	Beneficial effects
Dielectrophoresis: handling of gametes and embryos (positioning, manipulation, selection)	No formation of reactive oxygen species (centrifugation and washing of sperm) Non-invasive alternative to invasive gamete handling (pipetting, ICSI) No use of chemical agents upon parthenogenetic activation Alternative tool for morphological grading Non-invasive concentration of gametes: possible IVF for oligospermic patients
Electrowetting on dielectric: on-chip translation of nano- to microdroplets of culture medium (and/or reagents) with or without embryos/ gametes suspended within	Significantly smaller samples volume: more biomimetic, dynamic culture Reduction of reagents and processing time Viable mouse pups born after on-chip manipulation: full IVF cycle completed Exclusion of manual operations such as pipetting Efficient cf.-DNA extraction Chip reusability after cleaning/recoating Analysis of the secretome of a single embryo with no interference during IVC protocol Possible non-invasive alternative to PGS and PGD

processes and the requirements for the cell or medium of interest. Common issues associated with DEP devices are Joule heating, bubble formation, disrupted insulation and undesired reactions on the electrodes which may have a detrimental effect on the operation of the microchip. Furthermore, for successful DEP operation, a medium of low conductivity is required which adversely affects the viability of cells.<sup>86</sup> The known challenges related to the EWOD technology are the contact angle saturation and hysteresis.<sup>149,150</sup> Apart from these, the most common failure of the device is linked to electrolysis which can be observed as bubble formation within the chip. Low voltage EWOD is desirable, however, thinner insulators tend to break down upon applying an electric field. Another challenge in the construction of (D)MF chips handling biological samples are the changes of the surface properties due to the adsorption of molecules present in the culture medium.<sup>151,152</sup> This problem can be overcome with the use of surfactants.<sup>153–155</sup> However, these can be toxic to the different cell types or incompatible with the chip design. Evaporation of liquids which causes changes in the medium osmolarity is a separate issue which can negatively influence the *in vitro* development of mammalian embryos.<sup>156</sup> Additionally, differences in the early embryonic development among mammalian species exist,<sup>157</sup> so it seems reasonable to acknowledge other species as valuable models to decipher the paths involved in reproduction of mammals. Due to the ethical reasons concomitant with the culture of human embryos and stem cells, a regulation regarding the time of keeping these cells alive in *in vitro* culture was introduced. The so-called 14-day rule, only recently revised,<sup>158</sup> constituted for a substantial restriction on the studies regarding the processes involved in the conception, embryo implantation and gestation. Due to the novelty of the proposed techniques in *in vitro* manipulation of gametes and embryos, a lack of

standardization of protocols exists. The better the tools and more detailed the analysis of the cellular properties, the newer and more applicable models can be developed (as for example in<sup>120</sup>). More studies are necessary for the evaluation of the properties of these cells to draw a set of reference parameters for their *in vitro* handling. Such development is crucial for ARTs where the dominant method of the embryo and gamete assessment is based on the morphological grading. Lastly, the introduction of a novel apparatus exploiting phenomena such as DEP and EWOD requires training of personnel and a revision or adaptation of the existing protocols.

## Concluding remarks and future perspectives

Electrically stimulated microchips can be applied in assisted reproductive technologies to better mimic the *in vivo* surroundings of gametes and embryos as well as to understand the complexity of the processes involved in the early embryonic development, implantation and pregnancy. DEP can potentially be used for positioning, selection and guidance of gametes, microchannels of specific geometry for their confinement, EWOD for dynamic culture, medium refreshment and embryo assessment, while other embedded sensors could serve as tools for real-time evaluation of the embryo microenvironment *in vitro*. Developments in the synthesis of materials to better mimic the *in vivo* cellular microenvironment, such as hydrogels, and their on-chip incorporation are expected due to the high demand and suitability upon creating complex organ-on-chips. Taking into consideration the above-mentioned aspects along with the rapid expansion of (digital) microfluidics and its application in assisted reproductive technologies, a prototype of the full IVF-on-chip can be expected in the near future.



## Conflicts of interest

There are no conflicts to declare.

## Acknowledgements

This work was done in the frame of the project funded by Fonds Wetenschappelijk Onderzoek- Vlaanderen (FWO, project number G.0826.17N).

## References

- 1 M. Vander Borght and C. Wyns, Fertility and infertility: Definition and epidemiology, *Clin. Biochem.*, 2018, **62**, 2–10.
- 2 L. Thurston, A. Abbara and W. S. Dhillo, Investigation and management of subfertility, *J. Clin. Pathol.*, 2019, **72**, 579–587.
- 3 M. N. Mascarenhas, S. R. Flaxman, T. Boerma, S. Vanderpoel and G. A. Stevens, National, Regional, and Global Trends in Infertility Prevalence Since 1990: A Systematic Analysis of 277 Health Surveys, *PLoS Med.*, 2012, **9**, e1001356.
- 4 J. Fainberg and J. A. Kashanian, Recent advances in understanding and managing male infertility [version 1; peer review: 3 approved], *F1000Research*, 2019, **8**, 670.
- 5 F. Lotti and M. Maggi, Sexual dysfunction and male infertility, *Nat. Rev. Urol.*, 2018, **15**, 287–307.
- 6 C. Krausz and A. Riera-Escamilla, Genetics of male infertility, *Nat. Rev. Urol.*, 2018, **15**, 369–384.
- 7 R. B. Leaver, Male infertility: an overview of causes and treatment options, *Br. J. Nurs.*, 2016, **25**, S35–S40.
- 8 L. Biswas, K. Tyc, W. El Yakoubi, K. Morgan, J. Xing and K. Schindler, Meiosis interrupted: the genetics of female infertility via meiotic failure, *Reproduction*, 2021, **161**, R13–R35.
- 9 S. A. Yatsenko and A. Rajkovic, Genetics of human female infertility, *Biol. Reprod.*, 2019, **101**, 549–566.
- 10 R. S. Hussein, Z. Khan and Y. Zhao, Fertility Preservation in Women: Indications and Options for Therapy, *Mayo Clin. Proc.*, 2020, **95**, 770–783.
- 11 T. Tanbo and P. Fedoresak, Endometriosis-associated infertility: aspects of pathophysiological mechanisms and treatment options, *Acta Obstet. Gynecol. Scand.*, 2017, **96**, 659–667.
- 12 A. Cunha and A. M. Póvoa, Infertility management in women with polycystic ovary syndrome: a review, *Porto Biomed. J.*, 2021, **6**, e116.
- 13 J. T. Choy and M. L. Eisenberg, Male infertility as a window to health, *Fertil. Steril.*, 2018, **110**, 810–814.
- 14 B. Hanson, E. Johnstone, J. Dorais, B. Silver, C. M. Peterson and J. Hotaling, Female infertility, infertility-associated diagnoses, and comorbidities: a review, *J. Assist. Reprod. Genet.*, 2017, **34**, 167–177.
- 15 K. L. Rooney and A. D. Domar, The relationship between stress and infertility, *Dialogues Clin. Neurosci.*, 2018, **20**, 41–47.
- 16 F. Zegers-Hochschild, G. D. Adamson, S. Dyer, C. Racowsky, J. de Mouzon, R. Sokol, L. Rienzi, A. Sunde, L. Schmidt, I. D. Cooke, J. L. Simpson and S. van der Poel, The International Glossary on Infertility and Fertility Care, 2017, *Hum. Reprod.*, 2017, **32**, 1786–1801.
- 17 P. C. Steptoe and R. G. Edwards, Birth after the reimplantation of a human embryo, *Lancet*, 1978, **2**, 366.
- 18 J. D. Biggers, IVF and embryo transfer: Historical origin and development, *Reprod. BioMed. Online*, 2012, **25**, 118–127.
- 19 J. E. Swain, D. Carrell, A. Cobo, M. Meseguer, C. Rubio and G. D. Smith, Optimizing the culture environment and embryo manipulation to help maintain embryo developmental potential, *Fertil. Steril.*, 2016, **105**, 571–587.
- 20 K. Schulte, J. Ehmcke, S. Schlatt, M. Boiani and V. Nordhoff, Lower total cell numbers in mouse preimplantation embryos cultured in human assisted reproductive technique (ART) media are not induced by apoptosis, *Theriogenology*, 2015, **84**, 1620–1630.
- 21 L. B. Ferré, M. E. Kjelland, L. B. Strøbech, P. Hyttel, P. Mermilliod and P. J. Ross, Review: Recent advances in bovine in vitro embryo production: reproductive biotechnology history and methods, *Animal*, 2020, **14**, 991–1004.
- 22 Y. Sjunnesson, In vitro fertilisation in domestic mammals – a brief overview, *Upsala J. Med. Sci.*, 2020, **125**, 68–76.
- 23 B. Leemans, B. M. Gadella, T. A. E. Stout, C. De Schauwer, H. Nelis, M. Hoogewijs and A. Van Soom, Why doesn't conventional IVF work in the horse? The equine oviduct as a microenvironment for capacitation/fertilization, *Reproduction*, 2016, **152**, R233–R245.
- 24 F. A. García-Vázquez, C. Moros-Nicolás, R. López-Úbeda, E. Rodríguez-Tobón, A. Guillén-Martínez, J. W. Ross, C. Luongo, C. Matás, I. Hernández-Caravaca, M. Avilés and Ma J. Izquierdo-Rico, Evidence of haptoglobin in the porcine female genital tract during oestrous cycle and its effect on in vitro embryo production, *Sci. Rep.*, 2021, **11**, 12041.
- 25 E. París-Oller, S. Navarro-Serna, C. Soriano-Úbeda, J. S. Lopes, C. Matás, S. Ruiz, R. Latorre, O. López-Albors, R. Romar, S. Cánovas and P. Coy, Reproductive fluids, used for the in vitro production of pig embryos, result in healthy offspring and avoid aberrant placental expression of PEG3 and LUM, *J. Anim. Sci. Biotechnol.*, 2021, **12**, 32.
- 26 A. Asaadi, N. A. Dolatabad, H. Atashi, A. Raes, P. Van Damme, M. Hoelker, A. Hendrix, O. B. Pascottini, A. Van Soom, M. Kafi and K. C. Pavani, Extracellular vesicles from follicular and ampullary fluid isolated by density gradient ultracentrifugation improve bovine embryo development and quality, *Int. J. Mol. Sci.*, 2021, **22**, 578.
- 27 E. Wydooghe, L. Vandaele, S. Heras, P. De Sutter, D. Deforce, L. Peelman, C. De Schauwer and A. Van Soom, Autocrine embryotropins revisited: how do embryos



communicate with each other in vitro when cultured in groups?, *Biol. Rev.*, 2017, **92**, 505–520.

28 K. C. Pavani, C. Alminana, E. Wydooghe, M. Catteeuw, M. A. Ramírez, P. Mermilliod, D. Rizos and A. Van Soom, Emerging role of extracellular vesicles in communication of preimplantation embryos in vitro, *Reprod. Fertil. Dev.*, 2016, **29**, 66–83.

29 P. Coy, F. A. García-Vázquez, P. E. Visconti and M. Avilés, Roles of the oviduct in mammalian fertilization, *Reproduction*, 2012, **144**, 649–660.

30 S. Yuan, Z. Wang, H. Peng, S. M. Ward, G. W. Hennig, H. Zheng and W. Yan, Oviductal motile cilia are essential for oocyte pickup but dispensable for sperm and embryo transport, *Proc. Natl. Acad. Sci. U. S. A.*, 2021, **118**, e2102940118.

31 R. R. Santos, E. J. Schoevers and B. A. Roelen, Usefulness of bovine and porcine IVM/IVF models for reproductive toxicology, *Reprod. Biol. Endocrinol.*, 2014, **12**, 117.

32 G. M. Chambers, G. D. Adamson and M. J. C. Eijkemans, Acceptable cost for the patient and society, *Fertil. Steril.*, 2013, **100**, 319–327.

33 G. D. Adamson, Global cultural and socioeconomic factors that influence access to assisted reproductive technologies, *Women's Health*, 2009, **5**, 351–358.

34 M. C. Inhorn and P. Patrizio, Infertility around the globe: New thinking on gender, reproductive technologies and global movements in the 21st century, *Hum. Reprod. Update*, 2014, **21**, 411–426.

35 H. N. Sallam and N. H. Sallam, Religious aspects of assisted reproduction, *Facts Views Vis. Obgyn.*, 2016, **8**, 33–48.

36 P. Präg and M. C. Mills, Cultural determinants influence assisted reproduction usage in Europe more than economic and demographic factors, *Hum. Reprod.*, 2017, **32**, 2305–2314.

37 V. A. Kushnir, D. H. Barad, D. F. Albertini, S. K. Darmon and N. Gleicher, *Reprod. Biol. Endocrinol.*, 2017, **15**, 6.

38 N. Gleicher, V. A. Kushnir and D. H. Barad, Worldwide decline of IVF birth rates and its probable causes, *Hum. Reprod. Open*, 2019, **2019**, hoz017.

39 G. M. Chambers, V. P. Hoang, E. A. Sullivan, M. G. Chapman, O. Ishihara, F. Zegers-Hochschild, K. G. Nygren and G. D. Adamson, The impact of consumer affordability on access to assisted reproductive technologies and embryo transfer practices: an international analysis, *Fertil. Steril.*, 2014, **101**, 191–198.e4.

40 J. F. Kawnass and M. L. Badell, Maternal and fetal risk associated with assisted reproductive technology, *Obstet. Gynecol.*, 2018, **132**, 763–772.

41 B. Luke, Pregnancy and birth outcomes in couples with infertility with and without assisted reproductive technology: with an emphasis on US population-based studies, *Am. J. Obstet. Gynecol.*, 2017, **217**, 270–281.

42 M. Zgliczynska and K. Kosinska-Kaczynska, Micronutrients in multiple pregnancies—the knowns and unknowns: A systematic review, *Nutrients*, 2021, **13**, 386.

43 M. Sebghati and A. Khalil, Reduction of multiple pregnancy: Counselling and techniques, *Best Pract. Res. Clin. Obstet. Gynaecol.*, 2021, **70**, 112–122.

44 Z. Zheng, L. Chen, T. Yang, H. Yu, H. Wang and J. Qin, Multiple pregnancies achieved with IVF/ICSI and risk of specific congenital malformations: a meta-analysis of cohort studies, *Reprod. BioMed. Online*, 2018, **36**, 472–482.

45 S. Berntsen, V. Söderström-Anttila, U. B. Wennerholm, H. Laivuori, A. Loft, N. B. Oldereid, L. B. Romundstad, C. Bergh and A. Pinborg, The health of children conceived by ART: 'The chicken or the egg?', *Hum. Reprod. Update*, 2019, **25**, 137–158.

46 M. Chen and L. K. Heilbronn, The health outcomes of human offspring conceived by assisted reproductive technologies (ART), *J. Dev. Origins Health Dis.*, 2017, **8**, 388–402.

47 S. Mani and M. Mainigi, Embryo Culture Conditions and the Epigenome, *Semin. Reprod. Med.*, 2018, **36**, 211–220.

48 H. A. Stone, A. D. Stroock and A. Ajdari, Engineering flows in small devices: Microfluidics toward a lab-on-a-chip, *Annu. Rev. Fluid Mech.*, 2004, **36**, 381–411.

49 M. A. M. M. Ferraz, H. H. W. Henning, T. A. E. Stout, P. L. A. M. Vos and B. M. Gadella, Designing 3-Dimensional In Vitro Oviduct Culture Systems to Study Mammalian Fertilization and Embryo Production, *Ann. Biomed. Eng.*, 2017, **45**, 1731–1744.

50 L. Weng, IVF-on-a-Chip: Recent Advances in Microfluidics Technology for In Vitro Fertilization, *SLAS Technol.*, 2019, **24**, 373–385.

51 J. Hawkins, X. Miao, W. Cui and Y. Sun, Biophysical optimization of preimplantation embryo culture: What mechanics can offer ART, *Mol. Hum. Reprod.*, 2021, **27**, gaaa087.

52 B. Talebjedi, N. Tasnim, M. Hoorfar, G. F. Mastromonaco and M. De Almeida Monteiro Melo Ferraz, Exploiting Microfluidics for Extracellular Vesicle Isolation and Characterization: Potential Use for Standardized Embryo Quality Assessment, *Front. Vet. Sci.*, 2021, **7**, 620809.

53 A. B. Alias, H.-Y. Huang and D.-J. Yao, A Review on Microfluidics: An Aid to Assisted Reproductive Technology, *Molecules*, 2021, **26**, 4354.

54 G. D. Smith and S. Takayama, Application of microfluidic technologies to human assisted reproduction, *Mol. Hum. Reprod.*, 2017, **23**, 257–268.

55 S. Le Gac and V. Nordhoff, Microfluidics for mammalian embryo culture and selection: Where do we stand now?, *Mol. Hum. Reprod.*, 2017, **23**, 213–226.

56 A. N. Young, G. Moyle-Heyman, J. J. Kim and J. E. Burdette, Microphysiologic systems in female reproductive biology, *Exp. Biol. Med.*, 2017, **242**, 1690–1700.

57 R. C. Sequeira, T. Criswell, A. Atala and J. J. Yoo, Microfluidic Systems for Assisted Reproductive Technologies: Advantages and Potential Applications, *Tissue Eng. Regener. Med.*, 2020, **17**, 787–800.



58 M. B. Wheeler and M. Rubessa, Integration of microfluidics in animal in vitro embryo production, *Mol. Hum. Reprod.*, 2017, **23**, 248–256.

59 S. Thapa and Y. S. Heo, Microfluidic technology for in vitro fertilization (IVF), *JMST Adv.*, 2019, **1**, 1–11.

60 L. Z. Yanez and D. B. Camarillo, Microfluidic analysis of oocyte and embryo biomechanical properties to improve outcomes in assisted reproductive technologies, *Mol. Hum. Reprod.*, 2017, **23**, 235–247.

61 A. Nikshad, A. Aghlmandi, R. Safaralizadeh, L. Aghebati-Maleki, M. E. Warkaini, F. M. Khiavi and M. Yousefi, Advances of microfluidic technology in reproductive biology, *Life Sci.*, 2021, **265**, 118767.

62 R. Samuel, O. Badamjav, K. E. Murphy, D. P. Patel, J. Son, B. K. Gale, D. T. Carrell and J. M. Hotaling, Microfluidics: The future of microdissection TESE?, *Syst. Biol. Reprod. Med.*, 2016, **62**, 161–170.

63 K. L. Rappa, H. F. Rodriguez, G. C. Hakkarainen, R. M. Anchan, G. L. Mutter and W. Asghar, Sperm processing for advanced reproductive technologies: Where are we today?, *Biotechnol. Adv.*, 2016, **34**, 578–587.

64 S. S. Suarez and M. Wu, Microfluidic devices for the study of sperm migration, *Mol. Hum. Reprod.*, 2017, **23**, 227–234.

65 R. Nosrati, P. J. Graham, B. Zhang, J. Riordon, A. Lagunov, T. G. Hannam, C. Escobedo, K. Jarvi and D. Sinton, Microfluidics for sperm analysis and selection, *Nat. Rev. Urol.*, 2017, **14**, 707–730.

66 M. Štiavnická, L. Abril-Parreño, J. Nevoral, M. Králíčková and O. García-Álvarez, Non-invasive approaches to epigenetic-based sperm selection, *Med. Sci. Monit.*, 2017, **23**, 4677–4683.

67 M. Komeya, T. Sato and T. Ogawa, In vitro spermatogenesis: A century-long research journey, still half way around, *Reprod. Med. Biol.*, 2018, **17**, 407–420.

68 G. Marzano, M. S. Chiricàò, E. Primiceri, M. E. Dell'Aquila, J. Ramalho-Santos, V. Zara, A. Ferramosca and G. Maruccio, Sperm selection in assisted reproduction: A review of established methods and cutting-edge possibilities, *Biotechnol. Adv.*, 2020, **40**, 107498.

69 D. A. Vaughan and D. Sakkas, Sperm selection methods in the 21st century, *Biol. Reprod.*, 2019, **101**, 1076–1082.

70 C. L. Mangum, D. P. Patel, A. R. Jafek, R. Samuel, T. G. Jenkins, K. I. Aston, B. K. Gale and J. M. Hotaling, Towards a better testicular sperm extraction: novel sperm sorting technologies for non-motile sperm extracted by microdissection TESE, *Transl. Androl. Urol.*, 2020, **9**, S206–S214.

71 M. Khodamoradi, S. Rafizadeh Tafti, S. A. Mousavi Shaegh, B. Aflatoonian, M. Azimzadeh and P. Khashayar, Recent microfluidic innovations for sperm sorting, *Chemosensors*, 2021, **9**, 126.

72 M. Berenguel-Alonso, M. Sabés-Alsina, R. Morató, O. Ymber, L. Rodríguez-Vázquez, O. Talló-Parra, J. Alonso-Chamarro, M. Puyol and M. López-Béjar, Rapid Prototyping of a Cyclic Olefin Copolymer Microfluidic Device for Automated Oocyte Culturing, *SLAS Technol.*, 2017, **22**, 507–517.

73 L. Weng, G. Y. Lee, J. Liu, R. Kapur, T. L. Toth and M. M. Toner, On-chip oocyte denudation from cumulus-oocyte complexes for assisted reproductive therapy, *Lab Chip*, 2018, **18**, 3892–3902.

74 J. Gai, R. Nosrati and A. Neild, High DNA integrity sperm selection using surface acoustic waves, *Lab Chip*, 2020, **20**, 4262–4272.

75 S. Xiao, J. Riordon, M. Simchi, A. Lagunov, T. Hannam, K. Jarvi, R. Nosrati and D. Sinton, FertDish: microfluidic sperm selection-in-a-dish for intracytoplasmic sperm injection, *Lab Chip*, 2021, **21**, 775–783.

76 G. Vajta, T. Korösi, Y. Du, K. Nakata, S. Ieda, M. Kuwayama and Z. P. Nagy, The Well-of-the-Well system: An efficient approach to improve embryo development, *Reprod. BioMed. Online*, 2008, **17**, 73–81.

77 G. Zhao and J. Fu, Microfluidics for cryopreservation, *Biotechnol. Adv.*, 2017, **35**, 323–336.

78 K. Leonavicius, C. Royer, C. Preece, B. Davies, J. S. Biggins and S. Srinivas, Mechanics of mouse blastocyst hatching revealed by a hydrogel-based microdeformation assay, *Proc. Natl. Acad. Sci. U. S. A.*, 2018, **115**, 10375–10380.

79 L. Z. Yanez, J. Han, B. B. Behr, R. A. R. Pera and D. B. Camarillo, Human oocyte developmental potential is predicted by mechanical properties within hours after fertilization, *Nat. Commun.*, 2016, **7**, 10809.

80 M. G. Minasi, G. Fabozzi, V. Casciani, A. M. Lobascio, A. Colasante, F. Scarselli and E. Greco, Improved blastocyst formation with reduced culture volume: comparison of three different culture conditions on 1128 sibling human zygotes, *J. Assist. Reprod. Genet.*, 2015, **32**, 215–220.

81 P. Ramos-Ibeas, S. Heras, I. Gómez-Redondo, B. Planells, R. Fernández-González, E. Pericuesta, R. Laguna-Baraza, S. Pérez-Cerezales and A. Gutiérrez-Adán, Embryo responses to stress induced by assisted reproductive technologies, *Mol. Reprod. Dev.*, 2019, **86**, 1292–1306.

82 D. K. Gardner, R. Hamilton, B. McCallie, W. B. Schoolcraft and M. G. Katz-Jaffe, Human and mouse embryonic development, metabolism and gene expression are altered by an ammonium gradient in vitro, *Reproduction*, 2013, **146**, 49–61.

83 S. Chakraborty, Electrocapillary, in *Encyclopedia of Microfluidics and Nanofluidics*, ed. D. Li, Springer, Boston, MA, 2008, pp. 460–469.

84 Z. R. Gagnon, Cellular dielectrophoresis: Applications to the characterization, manipulation, separation and patterning of cells, *Electrophoresis*, 2011, **32**, 2466–2487.

85 B. Sarno, D. Heineck, M. J. Heller and S. D. Ibsen, Dielectrophoresis: Developments and applications from 2010 to 2020, *Electrophoresis*, 2021, **42**, 539–564.

86 N. A. Rahman, F. Ibrahim and B. Yafouz, Dielectrophoresis for Biomedical Sciences Applications: A Review, *Sensors*, 2017, **17**, 449.



87 F. Fontana, C. Rapone, G. Bregola, R. Aversa, A. de Meo, G. Signorini, M. Sergio, A. Ferrarini, R. Lanzellotto, G. Medoro, G. Giorgini, N. Minaresi and A. Berti, Isolation and genetic analysis of pure cells from forensic biological mixtures: The precision of a digital approach, *Forensic Sci. Int.: Genet.*, 2017, **29**, 225–241.

88 T. H. Lin and D. J. Yao, Applications of EWOD systems for DNA reaction and analysis, *J. Adhes. Sci. Technol.*, 2012, **26**, 1789–1804.

89 H. Wang, L. Chen and L. Sun, Digital microfluidics: A promising technique for biochemical applications, *Front. Mech. Eng.*, 2017, **12**, 510–525.

90 Y. P. Zhao and Y. Wang, Fundamentals and applications of electrowetting: A critical review, *Rev. Adhes. Adhes.*, 2013, **1**, 114–174.

91 K. Choi, A. H. C. Ng, R. Fobel and A. R. Wheeler, Digital microfluidics, *Annu. Rev. Anal. Chem.*, 2012, **5**, 413–440.

92 J. Li and C.-J. 'CJ' Kim, Current commercialization status of electrowetting-on-dielectric (EWOD) digital microfluidics, *Lab Chip*, 2020, **20**, 1705–1712.

93 E. Samiei, M. Tabrizian and M. Hoorfar, A review of digital microfluidics as portable platforms for lab-on-a-chip applications, *Lab Chip*, 2016, **16**, 2376–2396.

94 M. Alistar, Mobile microfluidics, *Bioengineering*, 2019, **6**, 5.

95 T. Kremers, S. Thelen, N. Bosbach and U. Schnakenberg, PortaDrop: A portable digital microfluidic platform providing versatile opportunities for Lab-On-A-Chip applications, *PLoS One*, 2020, **15**, e0238581.

96 D. Liu, Z. Yang, L. Zhang, M. Wei and Y. Lu, Cell-free biology using remote-controlled digital microfluidics for individual droplet control, *RSC Adv.*, 2020, **10**, 26972–26981.

97 M. Dhindsa, S. Kuiper and J. Heikenfeld, Reliable and low-voltage electrowetting on thin parylene films, *Thin Solid Films*, 2011, **519**, 3346–3351.

98 J. H. Kim, J.-H. Lee, J.-Y. Kim, A. Mirzaei, P. Wu, H. W. Kim and S. S. Kim, Electrowetting on dielectric (EWOD) properties of Teflon-coated electrosprayed silica layers in air and oil media and the influence of electric leakage, *J. Mater. Chem. C*, 2018, **6**, 6808–6815.

99 M. Khanna, S. Roy, A. Mathur, A. K. Dubey and R. Vashisth, Analysis of voltage distribution in electrowetting on Dielectric (EWOD) system, *Mater. Today: Proc.*, 2020, **38**, 179–185.

100 B. Koo and C. J. Kim, Evaluation of repeated electrowetting on three different fluoropolymer top coatings, *J. Micromech. Microeng.*, 2013, **23**, 067002.

101 H. A. Pohl, The motion and precipitation of suspensoids in divergent electric fields, *J. Appl. Phys.*, 1951, **22**, 869–871.

102 T. B. Jones, Basic Theory of Dielectrophoresis and Electrorotation, *IEEE Eng. Med. Biol. Mag.*, 2003, **22**, 33–42.

103 H. Morgan and N. Green, Dielectrophoresis, in *Encyclopedia of Microfluidics and Nanofluidics*, ed. D. Li, Springer, Boston, MA, 2008, pp. 350–357.

104 P. Benhal, D. Quashie, Y. Kim and J. Ali, Insulator Based Dielectrophoresis: Micro, Nano, and Molecular Scale Biological Applications, *Sensors*, 2020, **20**, 5095.

105 M. C. Wu, Optoelectronic Tweezers, *Nat. Photonics*, 2011, **5**, 322–324.

106 C. Quilliet and B. Berge, Electrowetting: A recent outbreak, *Curr. Opin. Colloid Interface Sci.*, 2001, **6**, 34–39.

107 G. Lippmann, Beziehungen zwischen den capillaren und elektrischen Erscheinungen, *Ann. Phys.*, 1873, **225**, 546–561.

108 G. Lippmann, Relations entre les phénomènes électriques et capillaires, *Ann. Chim. Phys.*, 1875, **5**, 494–549.

109 J. T. Stock, Gabriel Lippmann and the capillary electrometer, *Bull. Hist. Chem.*, 2004, **29**, 16–20.

110 S. K. Cho, H. Moon and C. J. Kim, Creating, transporting, cutting, and merging liquid droplets by electrowetting-based actuation for digital microfluidic circuits, *J. Microelectromech. Syst.*, 2003, **12**, 70–80.

111 Y. Y. Lin, E. R. F. Welch and R. B. Fair, Low voltage picoliter droplet manipulation utilizing electrowetting-on-dielectric platforms, *Sens. Actuators, B*, 2012, **173**, 338–345.

112 M. M. Nahar, J. B. Nikapitiya, S. M. You and H. Moon, Droplet velocity in an electrowetting on dielectric digital microfluidic device, *Micromachines*, 2016, **7**, 71.

113 N. Y. J. B. Nikapitiya, M. M. Nahar and H. Moon, Accurate, consistent, and fast droplet splitting and dispensing in electrowetting on dielectric digital microfluidics, *Micro Nano Syst. Lett.*, 2017, **5**, 24.

114 J. A. Mossman, J. T. Pearson, H. D. Moore and A. A. Pacey, Variation in mean human sperm length is linked with semen characteristics, *Hum. Reprod.*, 2013, **28**, 22–32.

115 K. S. Richter, D. C. Harris, S. T. Daneshmand and B. S. Shapiro, Quantitative grading of a human blastocyst: Optimal inner cell mass size and shape, *Fertil. Steril.*, 2001, **76**, 1157–1167.

116 J. L. Cavilla, C. R. Kennedy, A. G. Byskov and G. M. Hartshorne, Human immature oocytes grow during culture for IVM, *Hum. Reprod.*, 2008, **23**, 37–45.

117 L. Guzman, C. Ortega-Hrepich, F. K. Albuz, G. Verheyen, P. Devroey, J. Smitz and M. De Vos, Developmental capacity of in vitro-matured human oocytes retrieved from polycystic ovary syndrome ovaries containing no follicles larger than 6 mm, *Fertil. Steril.*, 2012, **98**, 503–507.e2.

118 P. Benhal, J. G. Chase, P. Gaynor, B. Oback and W. Wang, AC electric field induced dipole-based on-chip 3D cell rotation, *Lab Chip*, 2014, **14**, 2717–2727.

119 A. Q. Nguyen, I. Bardua, B. Greene, C. Wrenzycki, U. Wagner and V. Ziller, Mouse embryos exposed to oxygen concentrations that mimic changes in the oviduct and uterus show improvement in blastocyst rate, blastocyst size, and accelerated cell division, *Reprod. Biol.*, 2020, **20**, 147–153.

120 S. Shuchat, S. Park, S. Kol and G. Yossifon, Distinct and independent dielectrophoretic behavior of the head and tail



of sperm and its potential for the safe sorting and isolation of rare spermatozoa, *Electrophoresis*, 2019, **40**, 1606–1614.

121 E. Rosales-Cruzaley, P. A. Cota-Elizondo, D. Sánchez and B. H. Lapizco-Encinas, Sperm cells manipulation employing dielectrophoresis, *Bioprocess Biosyst. Eng.*, 2013, **36**, 1353–1362.

122 B. de Wagenaar, S. Dekker, H. L. de Boer, J. G. Bomer, W. Olthuis, A. van den Berg and L. I. Segerink, Towards microfluidic sperm refinement: impedance-based analysis and sorting of sperm cells, *Lab Chip*, 2016, **16**, 1514–1522.

123 J. B. Y. Koh and Marcos, Dielectrophoresis of spermatozoa in viscoelastic medium, *Electrophoresis*, 2015, **36**, 1514–1521.

124 T. Wongtawan, N. Dararatana, C. Thongkittidilok, S. Kornmatitsuk and B. Oonkhanond, Enrichment of bovine X-sperm using microfluidic dielectrophoretic chip: A proof-of-concept study, *Heliyon*, 2020, **6**, e05483.

125 A. T. Ohta, M. Garcia, J. K. Valley, L. Banie, H.-Y. Hsu, A. Jamshidi, S. L. Neale, T. Lue and M. C. Wu, Motile and non-motile sperm diagnostic manipulation using optoelectronic tweezers, *Lab Chip*, 2010, **10**, 3213–3217.

126 M. M. Garcia, A. T. Ohta, T. J. Walsh, E. Vittinghof, G. Lin, M. C. Wu and T. F. Lue, A noninvasive, motility independent, sperm sorting method and technology to identify and retrieve individual viable nonmotile sperm for intracytoplasmic sperm injection, *J. Urol.*, 2010, **184**, 2466–2472.

127 J. K. Valley, P. Swinton, W. J. Boscardin, T. F. Lue, P. F. Rinaudo, M. C. Wu and M. M. Garcia, Preimplantation Mouse Embryo Selection Guided by Light-Induced Dielectrophoresis, *PLoS One*, 2010, **5**, e10160.

128 K. Huang, I. A. Ajamieh, Z. Cui, J. Lai, J. K. Mills and H. K. Chu, Automated Embryo Manipulation and Rotation via Robotic nDEP-tweezers, *IEEE Trans. Biomed. Eng.*, 2021, **68**, 2152–2163.

129 H. Y. Huang, W. L. Kao, Y. W. Wang and D. J. Yao, Using a Dielectrophoretic Microfluidic Biochip Enhanced Fertilization of Mouse Embryo in Vitro, *Micromachines*, 2020, **11**, 714.

130 H. Y. Huang, Y. L. Lai and D. J. Yao, Dielectrophoretic Microfluidic Device for in Vitro Fertilization, *Micromachines*, 2018, **9**, 135.

131 H. Y. Huang, Y. H. Huang, W. L. Kao and D. J. Yao, Embryo formation from low sperm concentration by using dielectrophoretic force, *Biomicrofluidics*, 2015, **9**, 022404.

132 S. C. Méo, C. L. V. Leal and J. M. Garcia, Activation and early parthenogenesis of bovine oocytes treated with ethanol and strontium, *Anim. Reprod. Sci.*, 2004, **81**, 35–46.

133 P. J. Ross, Z. Beyhan, A. E. Iager, S. Y. Yoon, C. Malcuit, K. Schellander, R. A. Fissore and J. B. Cibelli, Parthenogenetic activation of bovine oocytes using bovine and murine phospholipase C zeta, *BMC Dev. Biol.*, 2008, **8**, 16.

134 E. Varga, R. Pataki, Z. Lorincz, J. Koltai and Á. B. Papp, Parthenogenetic development of in vitro matured porcine oocytes treated with chemical agents, *Anim. Reprod. Sci.*, 2008, **105**, 226–233.

135 R. Y. Yuan, F. Wang, S. Li, J. Y. Ma, L. Guo, X. L. Li, H. J. Zhu, X. Feng, Q. N. Li, Q. Zhou, Z. B. Lin, H. Schatten and X. H. Ou, Maturation conditions, post-ovulatory age, medium pH, and ER stress affect  $[Ca^{2+}]_i$  oscillation patterns in mouse oocytes, *J. Assist. Reprod. Genet.*, 2021, **38**, 1373–1385.

136 H. Y. Huang, W. L. Kao, Y. W. Wang and D. J. Yao, AC-electric-field-induced parthenogenesis of mouse oocyte, *Micro Nano Lett.*, 2018, **13**, 794–797.

137 A. L. Clow, P. T. Gaynor and B. J. Oback, A novel micropit device integrates automated cell positioning by dielectrophoresis and nuclear transfer by electrofusion, *Biomed. Microdevices*, 2010, **12**, 777–786.

138 H. Y. Huang, H. H. Shen, L. Y. Chung, Y. H. Chung, C. C. Chen, C. H. Hsu, S. K. Fan and D. J. Yao, Fertilization of Mouse Gametes in Vitro Using a Digital Microfluidic System, *IEEE Trans. Nanobioscience*, 2015, **14**, 857–863.

139 H. Y. Huang, H. H. Shen, C. H. Tien, C. J. Li, S. K. Fan, C. H. Liu, W. S. Hsu and D. J. Yao, Digital Microfluidic Dynamic Culture of Mammalian Embryos on an Electrowetting on Dielectric (EWOD) Chip, *PLoS One*, 2015, **10**, e0124196.

140 S. U. Son and R. L. Garrell, Transport of live yeast and zebrafish embryo on a droplet ('digital') microfluidic platform, *Lab Chip*, 2009, **9**, 2398–2401.

141 K. Henn and T. Braunbeck, Dechorionation as a tool to improve the fish embryo toxicity test (FET) with the zebrafish (*Danio rerio*), *Comp. Biochem. Physiol., Part C: Toxicol. Pharmacol.*, 2011, **153**, 91–98.

142 D. G. Pyne, J. Liu, M. Abdelgawad and Y. Sun, Digital Microfluidic Processing of Mammalian Embryos for Vitrification, *PLoS One*, 2014, **9**, e108128.

143 K. K. Ahuja and N. Macklon, Vitrification and the demise of fresh treatment cycles in ART, *Reprod. BioMed. Online*, 2020, **41**, 217–224.

144 A. B. Alias, C. E. Chiang, H. Y. Huang, K. T. Lin, P. J. Lu, Y. W. Wang, T. H. Wu, P. S. Jiang, C. A. Chen and D. J. Yao, Extraction of Cell-free Dna from An Embryo-culture Medium Using Micro-scale Bio-reagents on Ewod, *Sci. Rep.*, 2020, **10**, 9708.

145 C. E. Chiang, H. Y. Huang, K. T. Lin, A. B. Alias, P. J. Lu, Y. W. Wang, T. H. Wu, P. S. Jiang, C. A. Chen and D. J. Yao, A medical innovation: a new and improved method of DNA extraction with electrowetting-on-dielectric of genetic testing in-vitro fertilization (IVF), *Microfluid. Nanofluid.*, 2020, **24**, 55.

146 M. S. Lee, W. Hsu, H. Y. Huang, H. Y. Tseng, C. T. Lee, C. Y. Hsu, Y. C. Shieh, S. H. Wang, D. J. Yao and C. H. Liu, Simultaneous detection of two growth factors from human single-embryo culture medium by a bead-based



digital microfluidic chip, *Biosens. Bioelectron.*, 2020, **150**, 111851.

147 K. Sequeira, A. Espejel-Núñez, E. Vega-Hernández, A. Molina-Hernández and P. Grether-González, An increase in IL-1 $\beta$  concentrations in embryo culture-conditioned media obtained by in vitro fertilization on day 3 is related to successful implantation, *J. Assist. Reprod. Genet.*, 2015, **32**, 1623–1627.

148 S. O. Maslennikova, L. A. Gerlinskaya, G. V. Kontsevaya, M. V. Anisimova, S. A. Nedospasov, N. A. Feofanova, M. P. Moshkin and Y. M. Moshkin, TNF $\alpha$  is responsible for the canonical offspring number-size trade-off, *Sci. Rep.*, 2019, **9**, 4568.

149 F. Mugele, Fundamental challenges in electrowetting: From equilibrium shapes to contact angle saturation and drop dynamics, *Soft Matter*, 2009, **5**, 3377–3384.

150 W. C. Nelson, P. Sen and C. J. Kim, Dynamic contact angles and hysteresis under electrowetting-on-dielectric, *Langmuir*, 2011, **27**, 10319–10326.

151 Y. L. Jeyachandran, E. Mielczarski, B. Rai and J. A. Mielczarski, Quantitative and qualitative evaluation of adsorption/desorption of bovine serum albumin on hydrophilic and hydrophobic surfaces, *Langmuir*, 2009, **25**, 11614–11620.

152 H. T. M. Phan, S. Bartelt-Hunt, K. B. Rodenhausen, M. Schubert and J. C. Bartz, Investigation of Bovine Serum Albumin (BSA) Attachment onto Self-Assembled Monolayers (SAMs) Using Combinatorial Quartz Crystal Microbalance with Dissipation (QCM-D) and Spectroscopic Ellipsometry (SE), *PLoS One*, 2015, **10**, e0141282.

153 V. N. Luk, G. C. Mo and A. R. Wheeler, Pluronic Additives: A Solution to Sticky Problems in Digital Microfluidics, *Langmuir*, 2008, **24**, 6382–6389.

154 S. H. Au, P. Kumar and A. R. Wheeler, A New Angle on Pluronic Additives: Advancing Droplets and Understanding in Digital Microfluidics, *Langmuir*, 2011, **27**, 8586–8594.

155 I. Barbulovic-Nad, H. Yang, P. S. Park and A. R. Wheeler, Digital microfluidics for cell-based assays, *Lab Chip*, 2008, **8**, 519–526.

156 J. M. Baltz and A. P. Tartia, Cell volume regulation in oocytes and early embryos: connecting physiology to successful culture media, *Hum. Reprod. Update*, 2009, **16**, 166–176.

157 H. Shen, Embryo assembly 101, *Nature*, 2018, **559**, 19–22.

158 N. Subbaraman, Limit on lab-grown human embryos dropped, *Nature*, 2021, **594**, 18–19.

